Constraints on the density dependence of the symmetry energy

J. Łukasik
IFJ PAN, Kraków

IWM-EC 2018, Catania, 22-25.05.2018

Supported by Polish National Science Center, contract No. UMO-2017/25/B/ST2/02550

- short history and introduction
- present status
- future

Symmetry Energy (nucleus)

$$\frac{E_B}{A} = \underbrace{-a_V}_{Volume} + \underbrace{a_S \frac{1}{A^{1/3}}}_{Surface} + \underbrace{a_C \frac{Z^2}{A^{4/3}}}_{Coulomb} \underbrace{+ a_A \left(\frac{N-Z}{A}\right)^2}_{Symmetry} \pm \underbrace{a_P \frac{1}{A^{3/2}}}_{Pairing}$$

Binding Energy/Nucleon
(semiempirical
Bethe-Weizsäcker)
acc. better than 1%

a_V=15.8	a_S=18.0	a_C=0.72	a_A=23.5	a_P=11.5|0	[MeV]

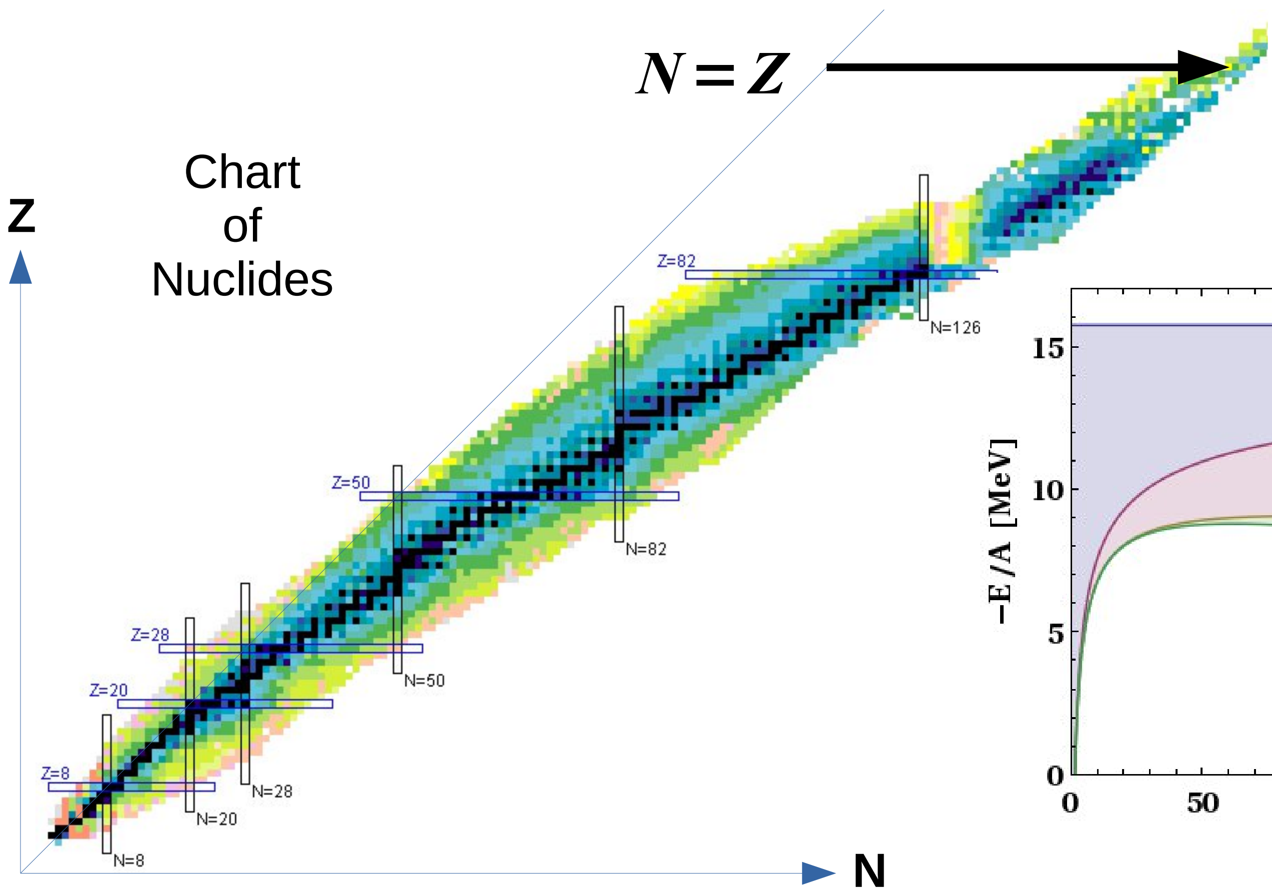

$$Z_\beta = \frac{A}{2 + A^{2/3} a_C / (2 a_A)}$$

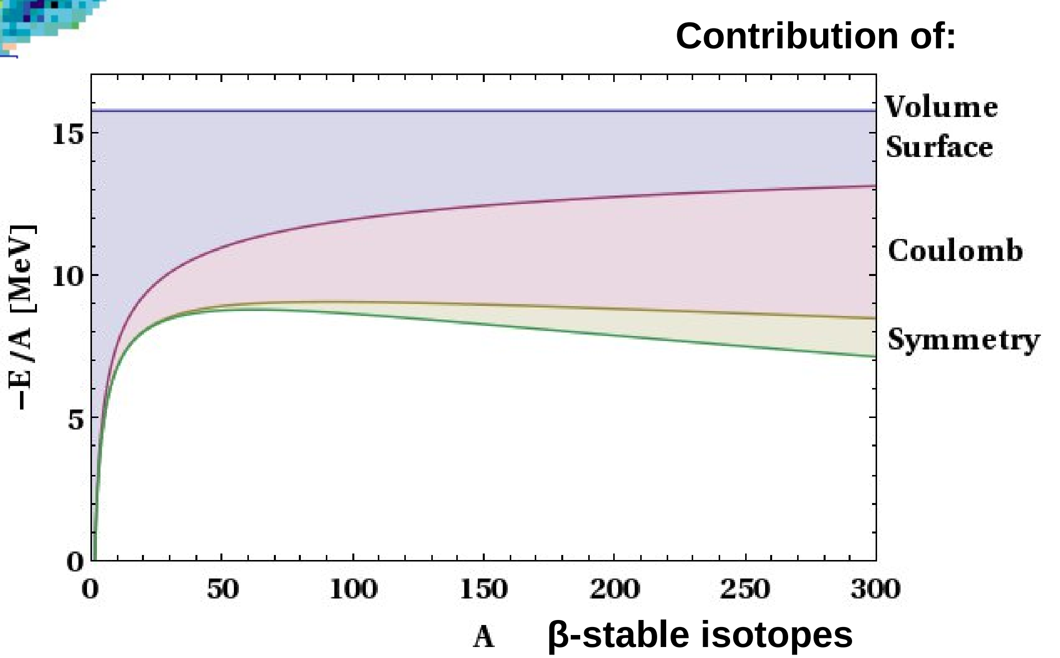

Symmetry Energy (nuclear matter)

$$\frac{E_B}{A} = \underbrace{-a_V}_{Volume} + \underbrace{a_S \frac{1}{A^{1/3}}}_{Surface} + \underbrace{a_C \frac{Z^2}{A^{4/3}}}_{Coulomb} \underbrace{+a_A \left(\frac{N-Z}{A}\right)^2}_{Symmetry} \underbrace{\pm a_P \frac{1}{A^{3/2}}}_{Pairing}$$

Energy per nucleon in nuclear matter (EoS):

$$E(\rho, \delta) = E(\rho, 0) + E_{sym}(\rho)\,\delta^2 + o(\delta^4)$$

dominant symmetric matter (N=Z) term (*isoscalar*):

$$E(\rho, 0) \approx -a_V + \frac{K}{18}\left(\frac{\rho-\rho_o}{\rho_o}\right)^2 + \cdots$$

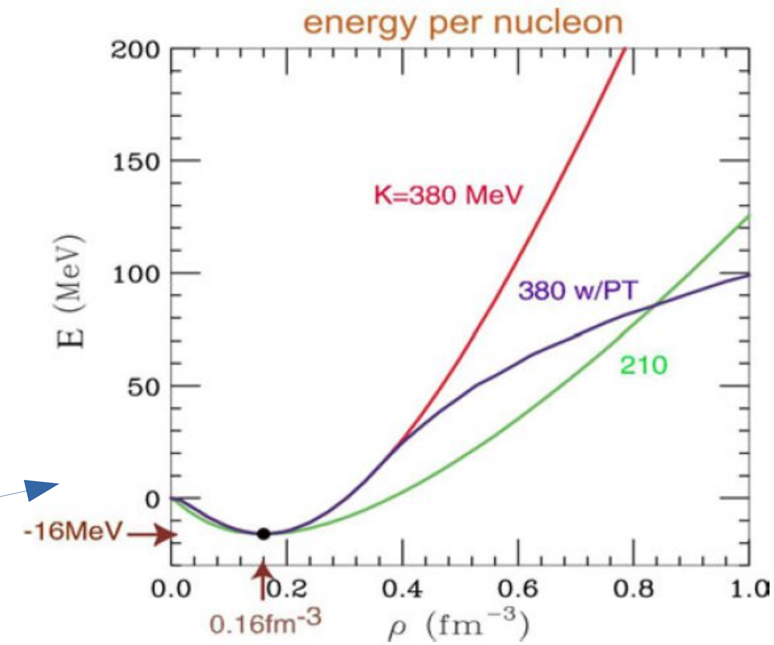

P. Danielewicz, arXiv:nucl-th/0512009

symmetry term (*isovector*):

$$E_{sym}(\rho) \approx E_{sym}(\rho_0) + \frac{L}{3}\left(\frac{\rho-\rho_o}{\rho_o}\right) + \frac{K_{sym}}{18}\left(\frac{\rho-\rho_o}{\rho_o}\right)^2 + \cdots$$

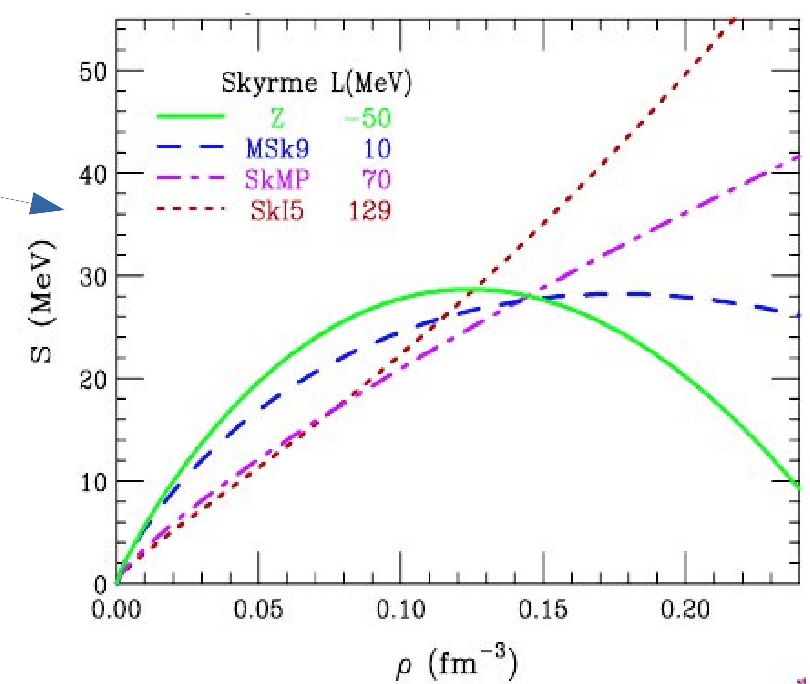

(*)P. Danielewicz, J. Lee, NPA 818(2009)36

ρ_n, ρ_p → neutron, proton densities

$\rho = \rho_n + \rho_p$ → nucleon density

$\delta = \frac{\rho_n - \rho_p}{\rho}$ → isospin asymmetry

$L = 3\rho_o \left.\frac{\partial E_{sym}}{\partial \rho}\right|_{\rho=\rho_o}$ → ~ symmetry pressure

$K = 9\rho_o^2 \left.\frac{\partial^2 E}{\partial \rho^2}\right|_{\rho=\rho_o}$ → compressibility

Symmetry Energy (nuclear matter)

$$\frac{E_B}{A} = \underbrace{-a_V}_{Volume} + \underbrace{a_S \frac{1}{A^{1/3}}}_{Surface} + \underbrace{a_C \frac{Z^2}{A^{4/3}}}_{Coulomb} \underbrace{+ a_A \left(\frac{N-Z}{A}\right)^2}_{Symmetry} \pm \underbrace{a_P \frac{1}{A^{3/2}}}_{Pairing}$$

Energy per nucleon in nuclear matter (EoS):

$$E(\rho,\delta) = E(\rho,0) + E_{sym}(\rho)\,\delta^2 + o(\delta^4)$$

dominant symmetric matter (N=Z) term (*isoscalar*):

$$E(\rho,0) \approx -a_V + \frac{K}{18}\left(\frac{\rho-\rho_o}{\rho_o}\right)^2 + \cdots$$

symmetry term (*isovector*):

$$E_{sym}(\rho) \approx E_{sym}(\rho_0) + \frac{L}{3}\left(\frac{\rho-\rho_o}{\rho_o}\right) + \frac{K_{sym}}{18}\left(\frac{\rho-\rho_o}{\rho_o}\right)^2 + \cdots$$

ρ_n, ρ_p → neutron, proton densities

$\rho = \rho_n + \rho_p$ → nucleon density

$\delta = \frac{\rho_n - \rho_p}{\rho}$ → isospin asymmetry

$L = 3\rho_o \left.\frac{\partial E_{sym}}{\partial \rho}\right|_{\rho=\rho_o}$ → ~symmetry pressure

$K = 9\rho_o^2 \left.\frac{\partial^2 E}{\partial \rho^2}\right|_{\rho=\rho_o}$ → compressibility

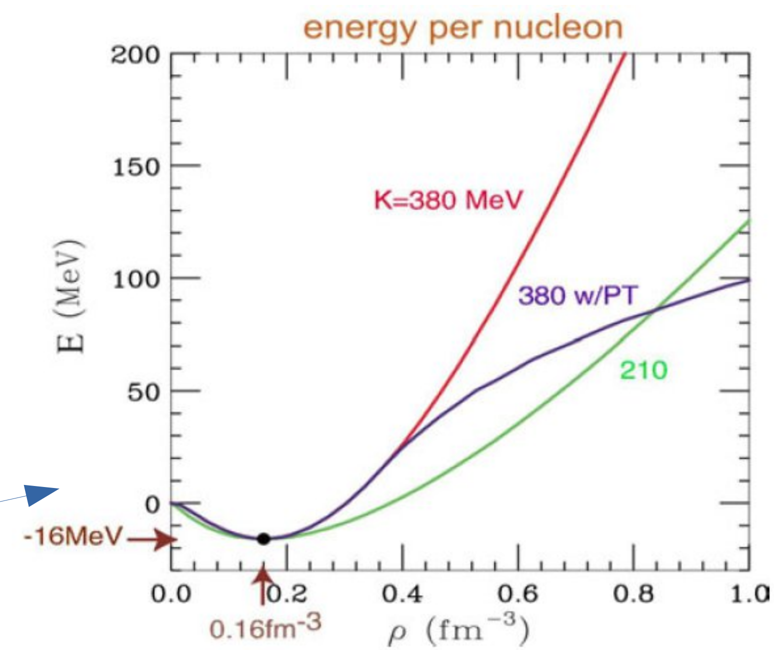

P. Danielewicz, arXiv:nucl-th/0512009

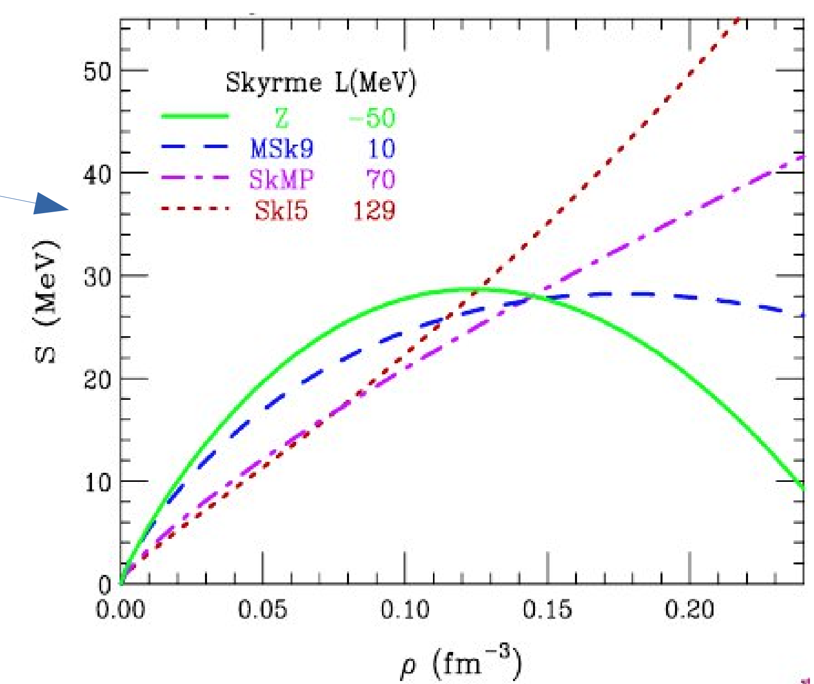

(*)P. Danielewicz, J. Lee, NPA 818(2009)36

More exact formula

B.-A. Li, Nucl. Phys. News, 27 (2017) 7

It is well known that the nucleon potential $U_{n/p}(k,\rho,\delta)$ in ANM can be expanded up to the second order in δ as

$$U_\tau(k,\rho,\delta) = U_0(k,\rho) + \tau_3 U_{sym,1}(k,\rho)\cdot\delta + U_{sym,2}(k,\rho)\cdot\delta^2 + \mathcal{O}(\delta^3), \qquad (2)$$

where $\tau_3 = \pm$ for $\tau = n/p$ and $U_0(k,\rho)$, $U_{sym,1}(k,\rho)$ and $U_{sym,2}(k,\rho)$ are the isoscalar, isovector (symmetry or Lane potential [15]) and the second-order isoscalar potentials, respectively. At the mean-field level, using the Bruckner theory [16, 17] or the Hugenholtz-Van Hove (HVH) theorem [18], the $E_{sym}(\rho)$ and its density slope $L(\rho) \equiv [3\rho(\partial E_{sym}/\partial\rho)]_\rho$ at an arbitrary density ρ can be expressed generally as [19–21]

$$E_{sym}(\rho) = \frac{1}{3}\frac{\hbar^2 k_F^2}{2m_0^*} + \frac{1}{2}U_{sym,1}(\rho,k_F), \qquad (3)$$

$$L(\rho) = \frac{2}{3}\frac{\hbar^2 k_F^2}{2m_0^*} + \frac{3}{2}U_{sym,1}(\rho,k_F) - \frac{1}{6}\left(\frac{\hbar^2 k^3}{m_0^{*2}}\frac{\partial m_0^*}{\partial k}\right)|_{k_F} + \frac{dU_{sym,1}}{dk}|_{k_F} k_F + 3U_{sym,2}(\rho,k_F), \qquad (4)$$

where $k_F = (3\pi^2\rho/2)^{1/3}$ is the nucleon Fermi momentum and $m_0^*/m = (1 + \frac{m}{\hbar^2 k_F} dU_0/dk)^{-1}|_{k_F}$ is the nucleon isoscalar effective mass. The $E_{sym}(\rho)$ consists of two terms, i.e., the kinetic symmetry energy $E^1_{sym}(\rho)$ equivalent to 1/3 the Fermi energy of quasi-nucleons with an isoscalar effective mass m_0^* and the potential symmetry energy $E^2_{sym}(\rho)$ equivalent to 1/2 the isovector potential $U_{sym,1}(\rho,k_F)$ at k_F. The density slope $L(\rho)$ can be cast into five terms

It is important to point out that the $E_{sym}(\rho)$ is closely related to the neutron-proton effective mass splitting $m^*_{n-p} \equiv (m^*_{\rm n} - m^*_{\rm p})/m$, which is a fundamental quantity having broad impacts on many interesting issues in both nuclear physics and astrophysics [23, 24]. In terms of the momentum dependence of the single-nucleon potential or the $E_{sym}(\rho)$ and $L(\rho)$, one has

$$m^*_{n-p} \approx \frac{2\delta m}{\hbar^2 k_F}\left[-\frac{dU_{sym,1}}{dk} - \frac{k_F}{3}\frac{d^2U_0}{dk^2} + \frac{1}{3}\frac{dU_0}{dk}\right]\left(\frac{m_0^*}{m}\right)^2 \approx \frac{\delta}{E_F(\rho)}\left[3E_{sym}(\rho) - L(\rho) - \frac{1}{3}\frac{m}{m_0^*}E_F(\rho)\right]\left(\frac{m_0^*}{m}\right)^2$$

where $E_F(\rho)$ is the Fermi energy in SNM at density ρ. Therefore, while probing the density dependence of the nuclear symmetry energy, we are also studying the neutron-proton effective mass splitting in neutron-rich nuclear matter [23–25].

K for symmetric matter (δ=0)

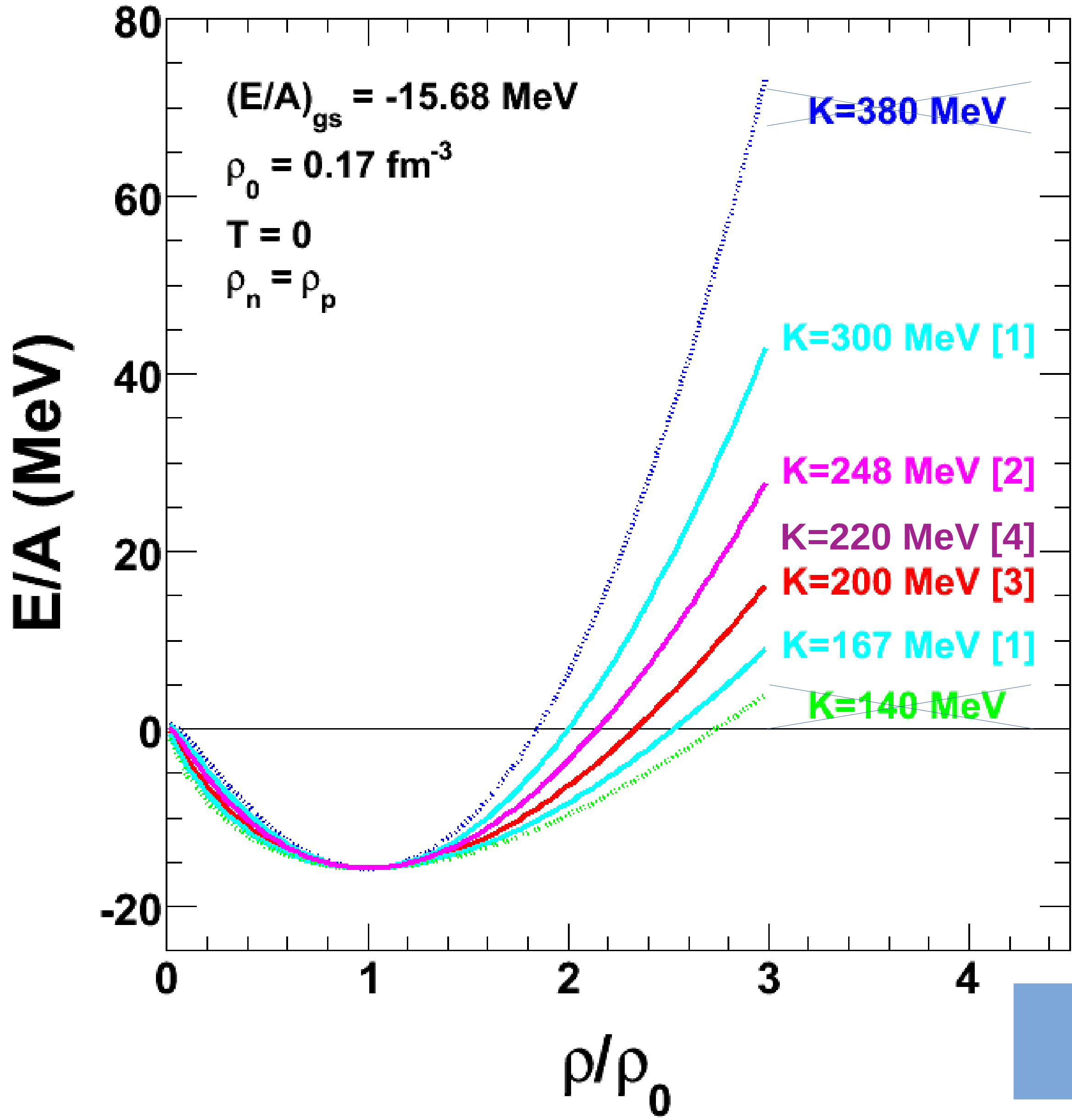

[1] Flow:
P. Danielewicz et al., Science 298 (02) 1592
BME: K = 167-300 MeV

[2] ISGMR:
J. Piekarewicz, PRC 69 (04) 041301
RMF: K=248 MeV
G. Colò et al.,PRC 70 (04) 024307
Skyrme HF: K=230 MeV
S. Shlomo, et al. Eur. Phys. J. A 30, 23 (2006)
K = 240 ± 20 MeV

[3] Subtreshold K^+:
C. Sturm et al., PRL 86 (01) 39
Ch. Hartnack et al., PRL 96 (06) 012302
Flow:
W. Reisdorf (FOPI) arXiv:1307.4210 [nucl-ex]
IQMD: K=200 MeV

[4] Y. Wang et al., PLB 778 (2018) 207
UrQMD + FOPI: K = 220 ± 40 MeV

"Generally accepted" value of
K = 240 ± 20 MeV

Symmetry term. Why so uncertain?

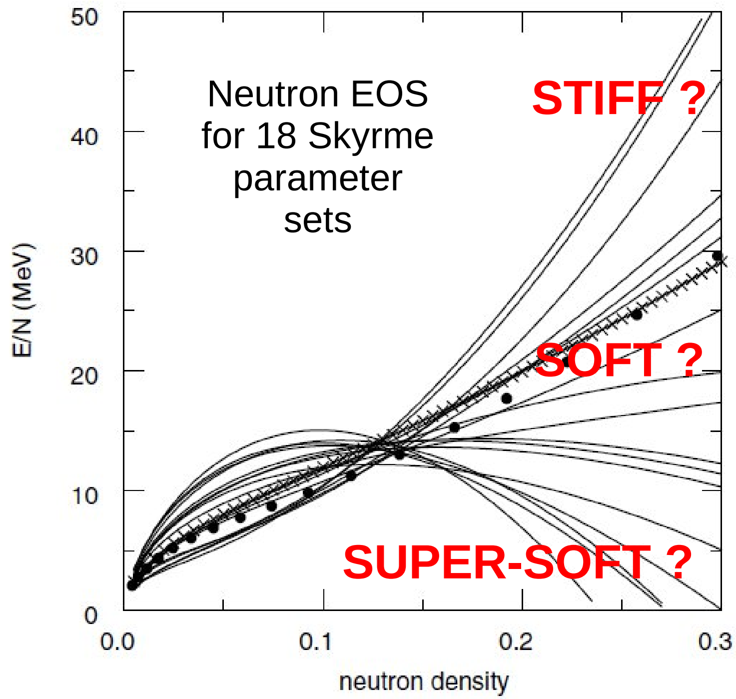

B. Alex Brown, PRL 85(2000)5296

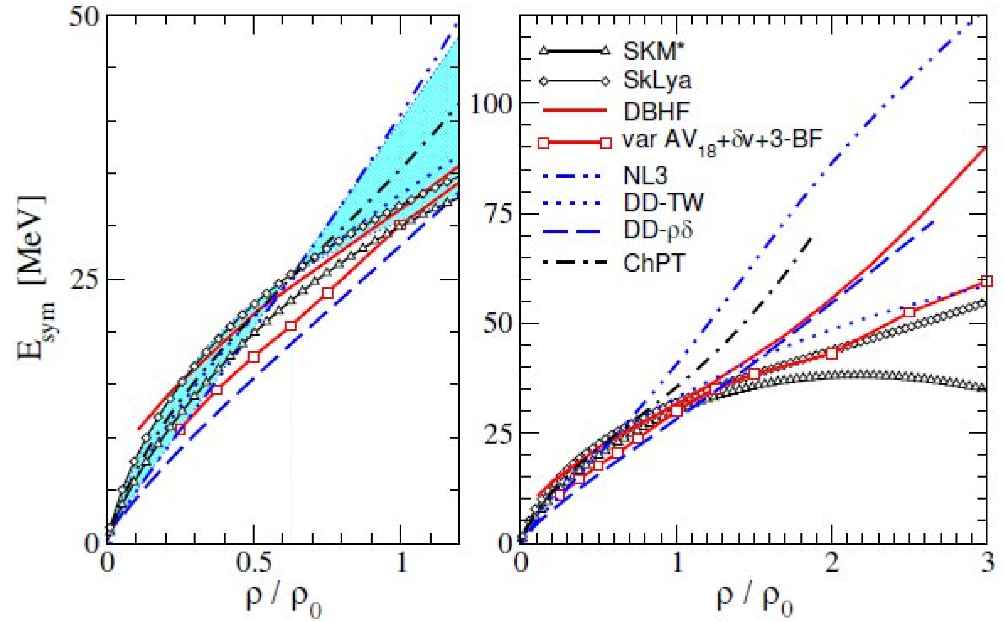

C. Fuchs and H.H. Wolter, EPJA 30(2006)5

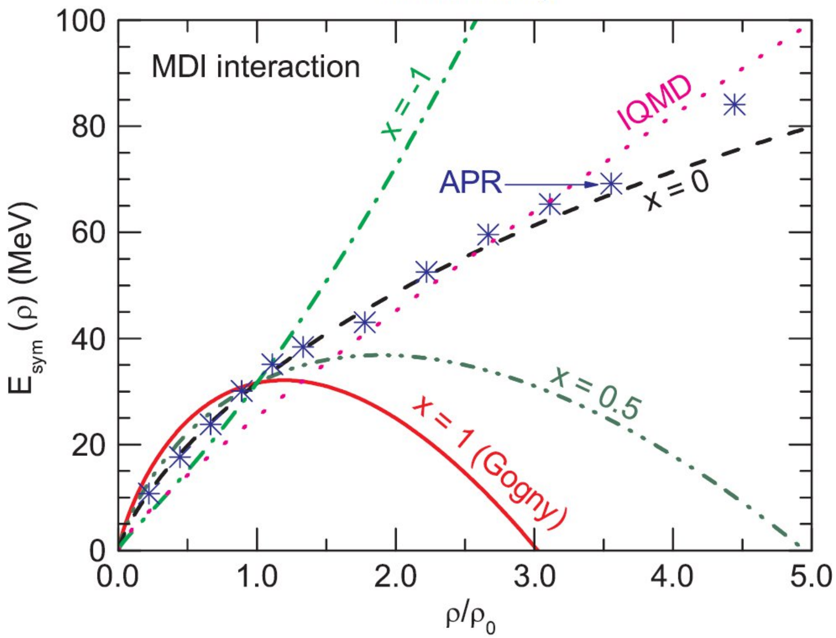

Z. Xiao et al., PRL 102(2009)062502

Symmetry energy uncertain at high density and modified by clustering at low density

Phenomenological forces constrained around saturation and for nearly isospin-symmetric matter. Poor knowledge of effective forces in neutron-rich matter. Uncertainties in the nature of the three-neutron force. Uncertain extrapolations above the saturation density.

Why so important?

ASTROPHYSICS

- Neutron star structure, composition, size, mass and cooling rate, crust-core transition density
- Pulsars, masses, spin rates
- Supernova explosions
- Stellar nucleosynthesis, r-process

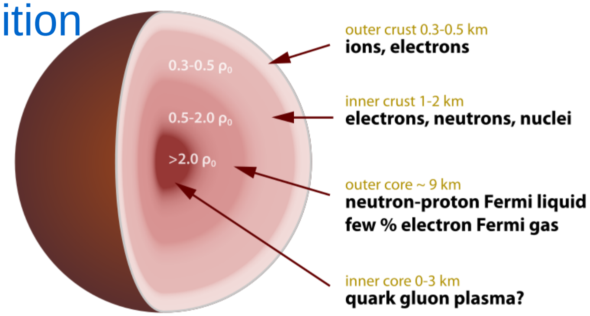

Robert Schulze (Wikipedia)

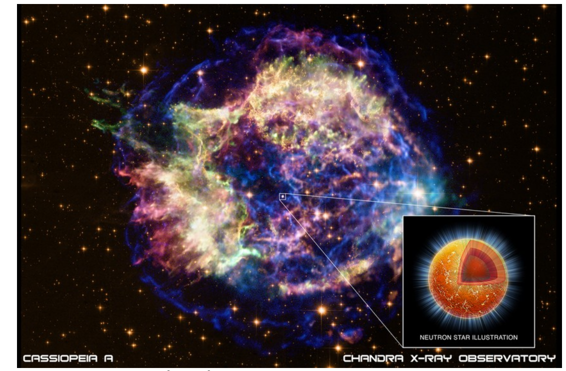

Cassiopeia A Supernova Remnant
(http://chandra.harvard.edu/photo/printgallery/2004/)

STRUCTURE

- Structure of exotic nuclei (masses, drip lines)
- Neutron skin thickness
- IvGDR
- Pygmy resonances
- Differences between IAS

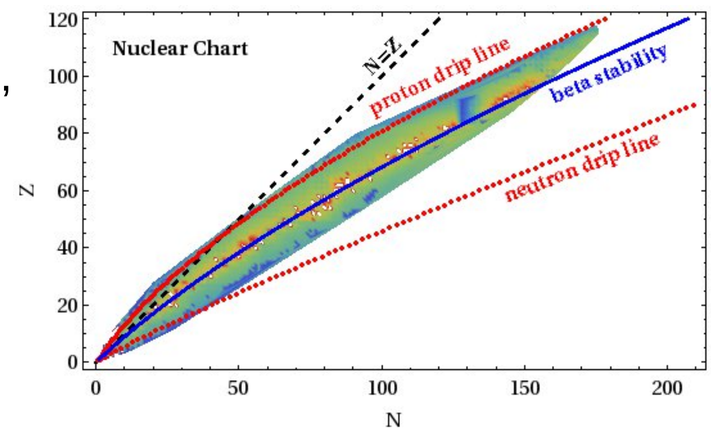

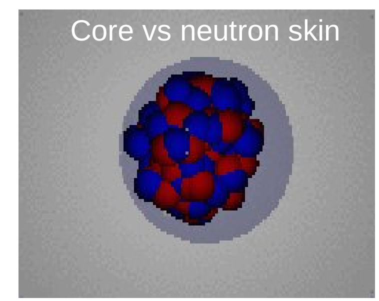

PDR

REACTIONS

- Flow patterns in HIC
- Multifragmentation, isoscaling, isospin diffusion
- n/p, t/^{3}He, π^-/π^+, K^+/K^0 ratios in HIC

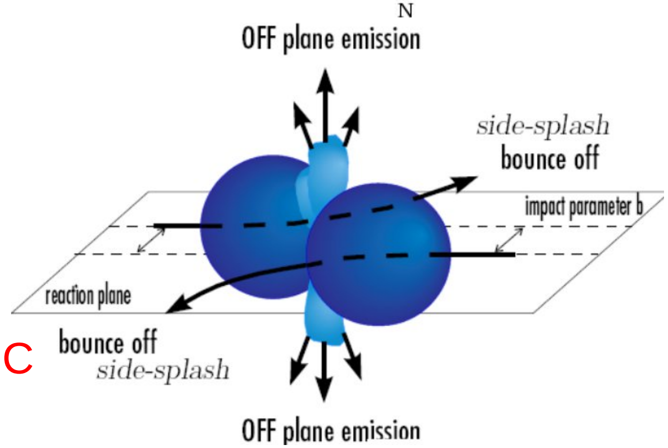

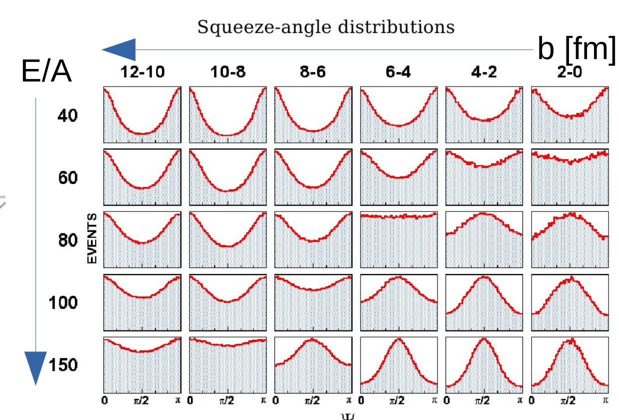

Au+Au

The Mass & Radius of Neutron Stars

from qLMXB

A “nuclear diesel”

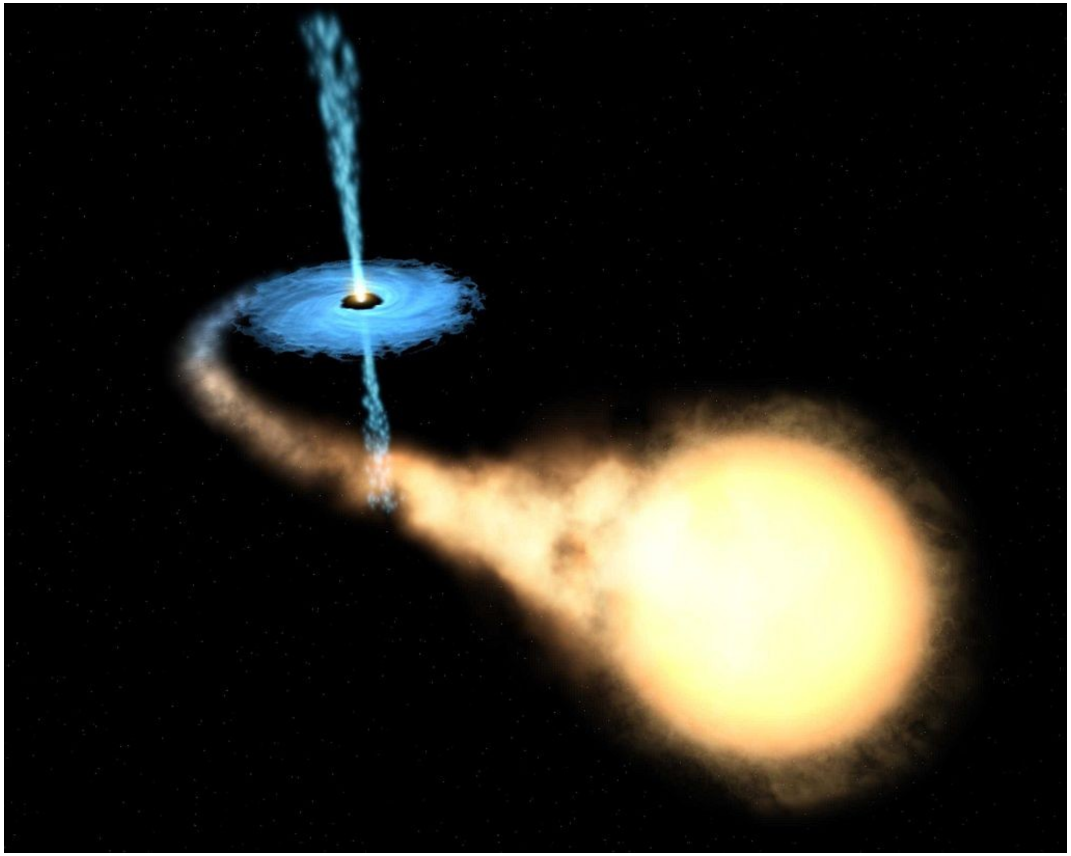

The Mass & Radius of Neutron Stars

from qLMXB

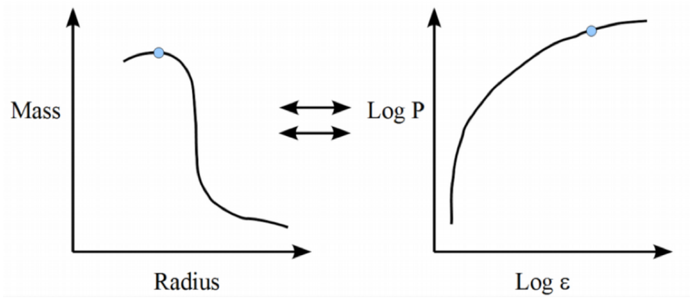

Guillot et al. (2013)

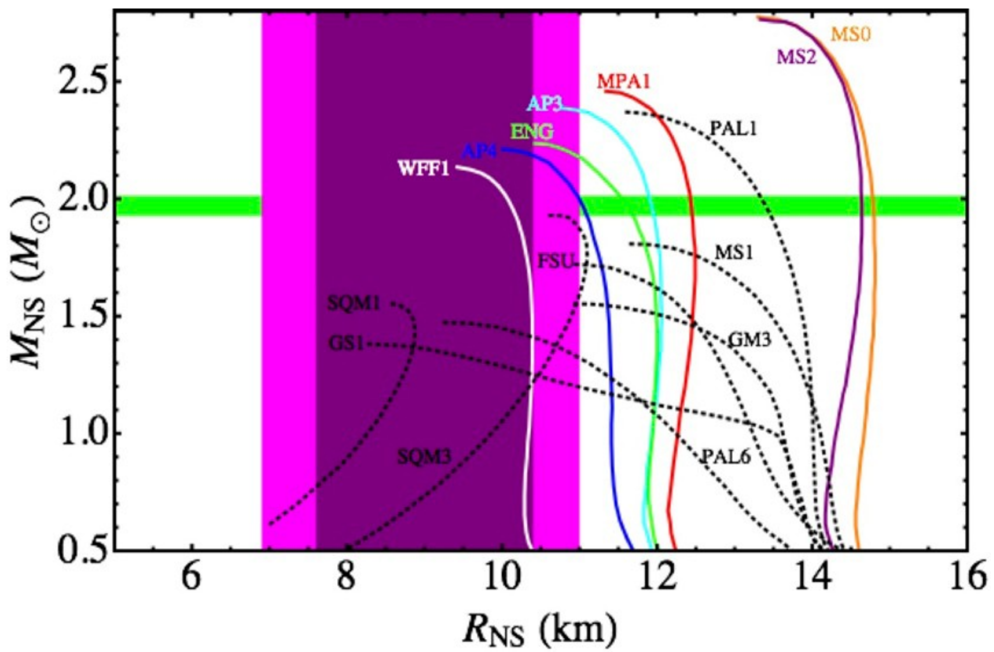

$$R_{\mathrm{NS}} = 9.1^{+1.3}_{-1.5}\ \mathrm{km}\ (90\%\text{-confidence})$$

WFF1: $E_{sym} \approx 26$ MeV, L ≈ 60 MeV

Lattimer & Steiner (2013)

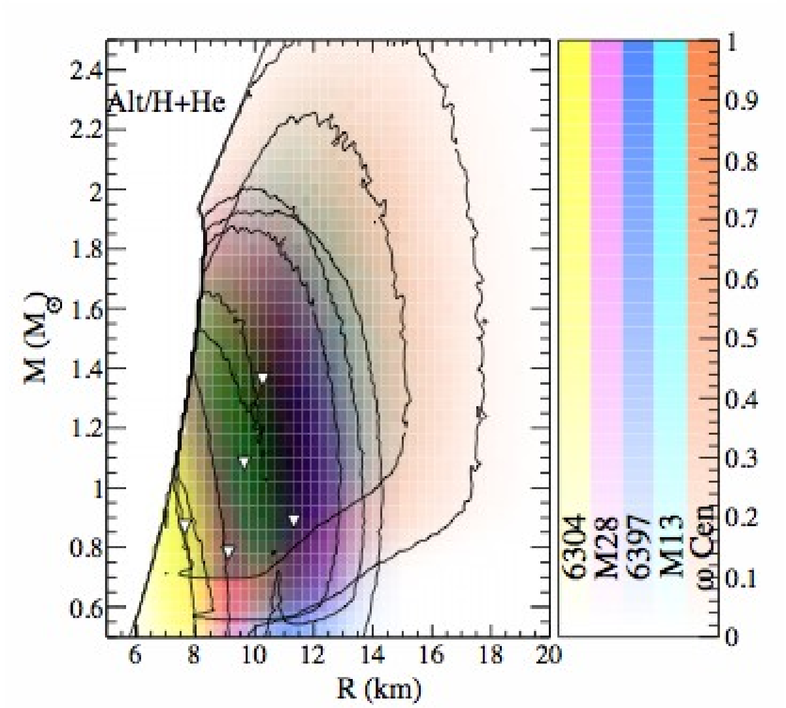

$$10.9 < R_{NS} < 12.7\ \mathrm{km}\ (2.0\ M_\odot)$$

41 < L < 83 MeV

(analysis of the same data)

The Mass & Radius of Neutron Stars

from qLMXB

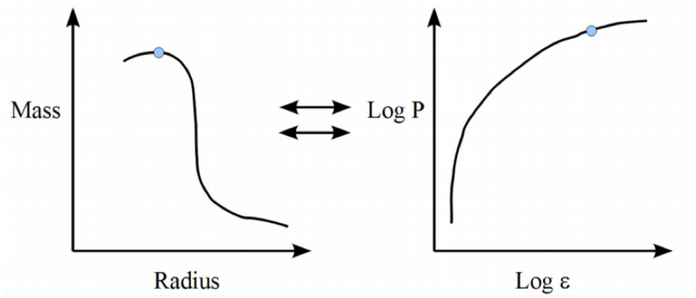

Guillot et al., ApJ 772, 7 (2013)

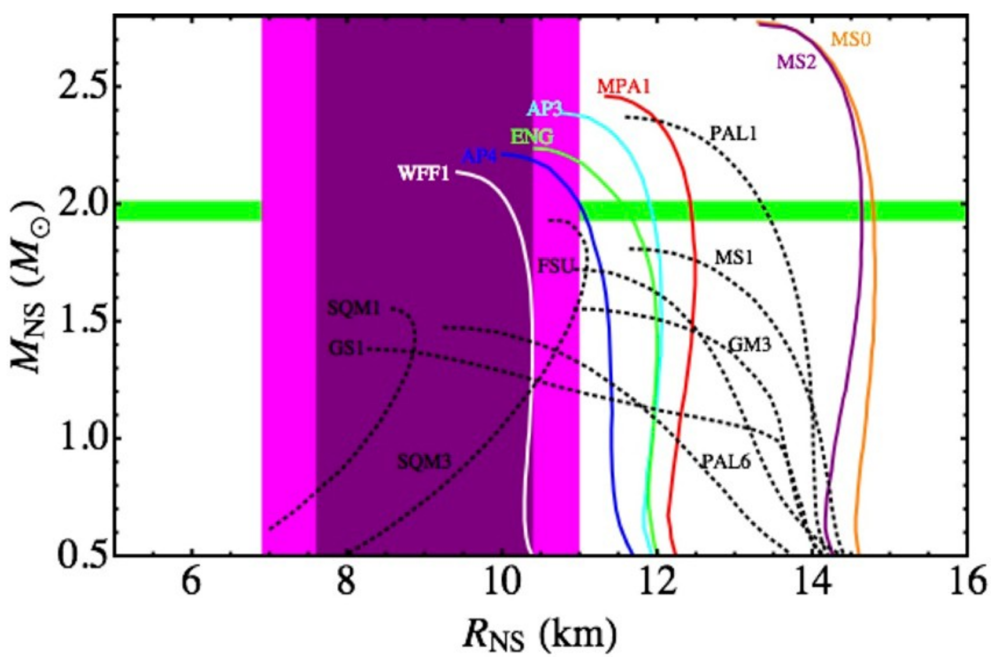

$$R_{NS} = 9.1^{+1.3}_{-1.5}\ \text{km (90\%-confidence)}$$

WFF1: $E_{sym} \approx 26$ MeV, L ≈ 60 MeV

Lattimer & Steiner (2013)

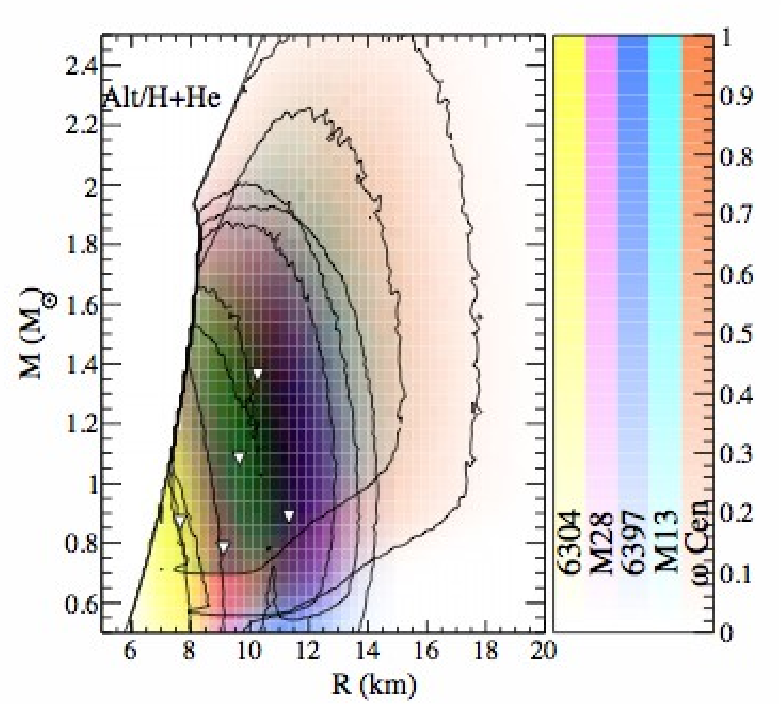

$$10.9 < R_{NS} < 12.7\ \text{km}\ (2.0\ M_\odot)$$

41 < L < 83 MeV

updates

S. Guillot et al. ApJL, 796:L3,2014: R_{NS} = 9.4 ± 1.2 km

F. Özel et al., ApJ, 820:28,2016: R_{NS} = 10.1-11.1 km (1.5 $M_\odot$)

A.W. Shaw at al., arXiv:1803.00029 [astro-ph.HE]

$$R_{NS} = 12^{+1.9}_{-1.7}\, km\, (1.4\, M_\odot)$$

current status

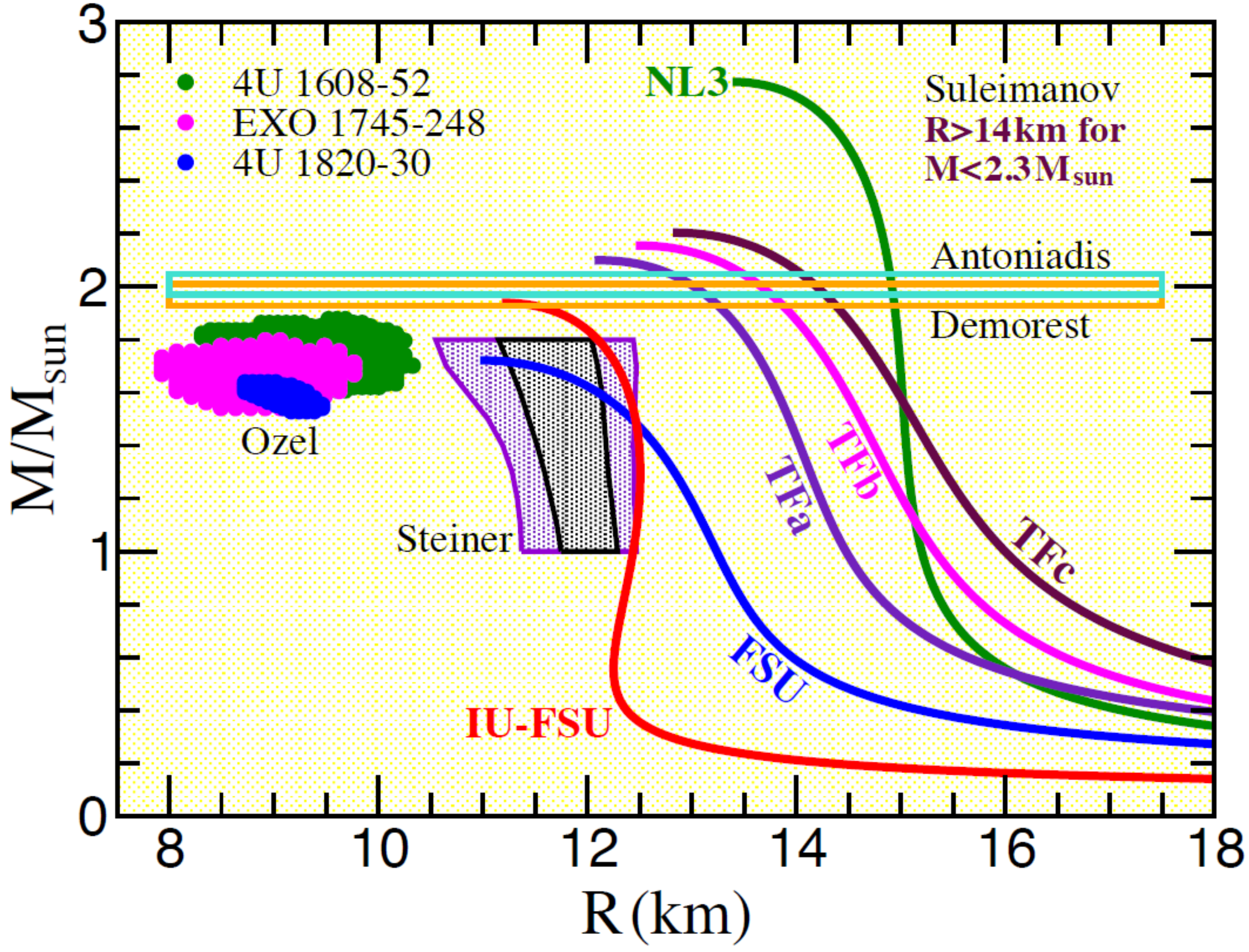

J. Piekarewicz, arXiv:1805.04780v1

current status

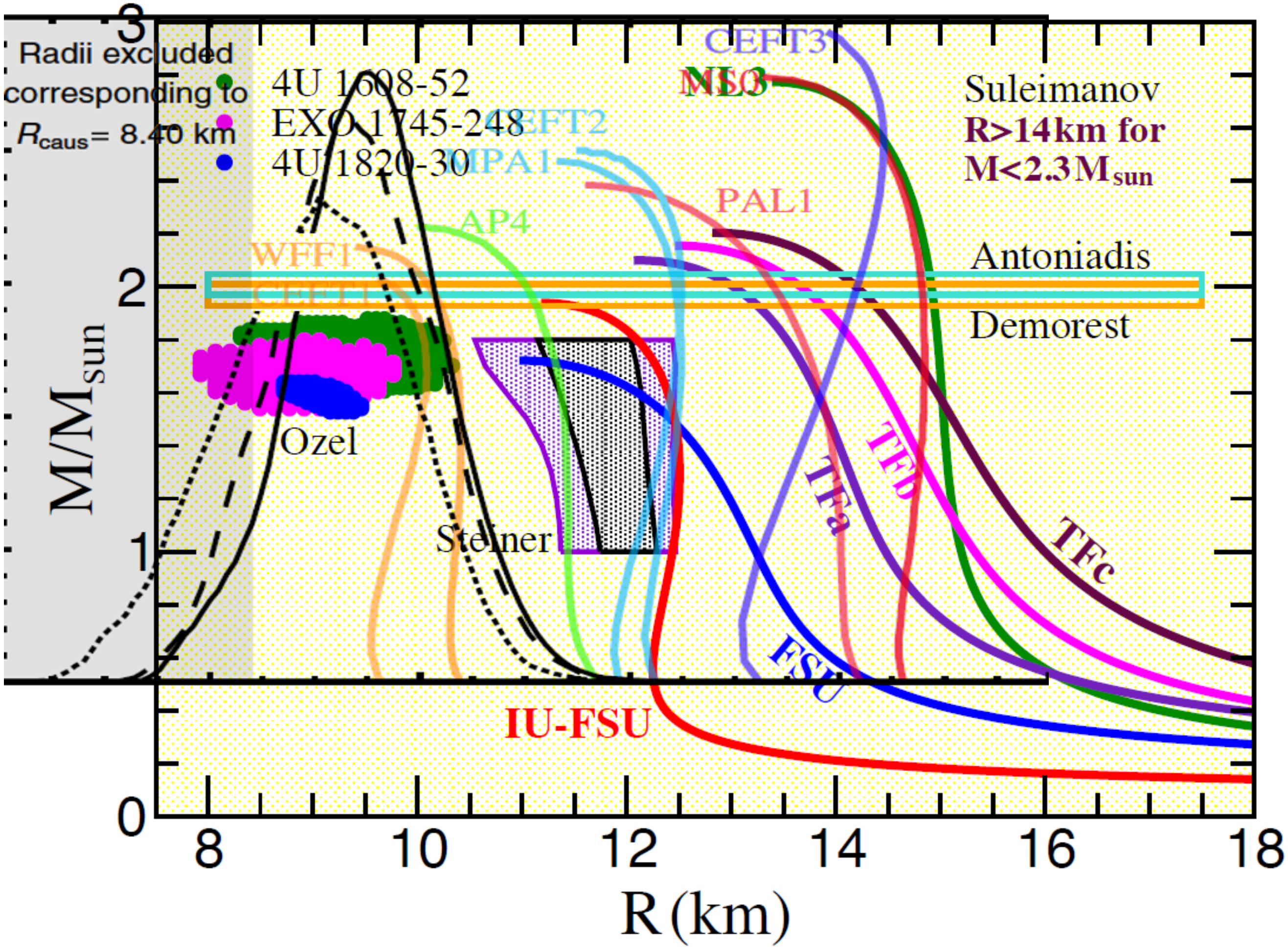

J. Piekarewicz, arXiv:1805.04780v1 + S. Guillot and R. Rutlege, AJL 796:L3(2014)

Waltzing Neutron Stars shaking the Universe

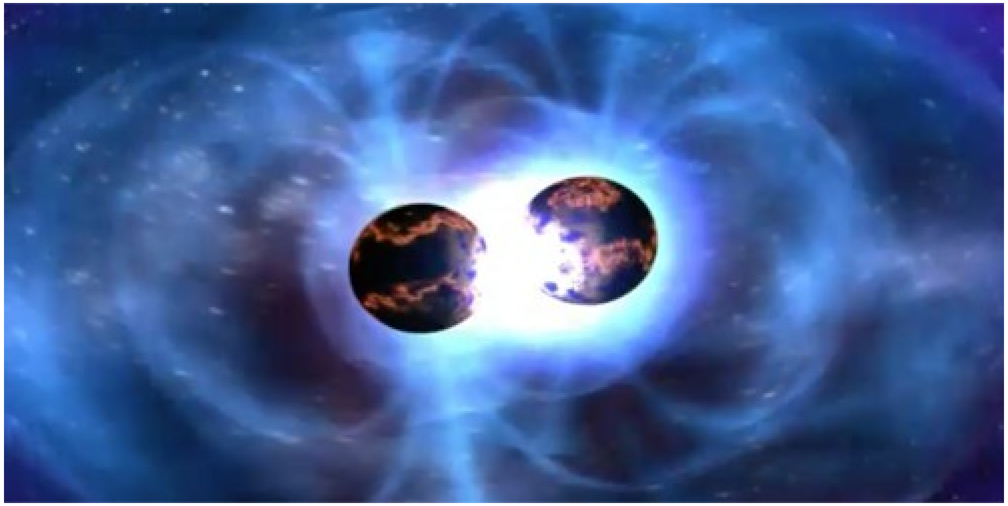

NASA/Goddard Space Flight Center

Gravitational Wave Constraints

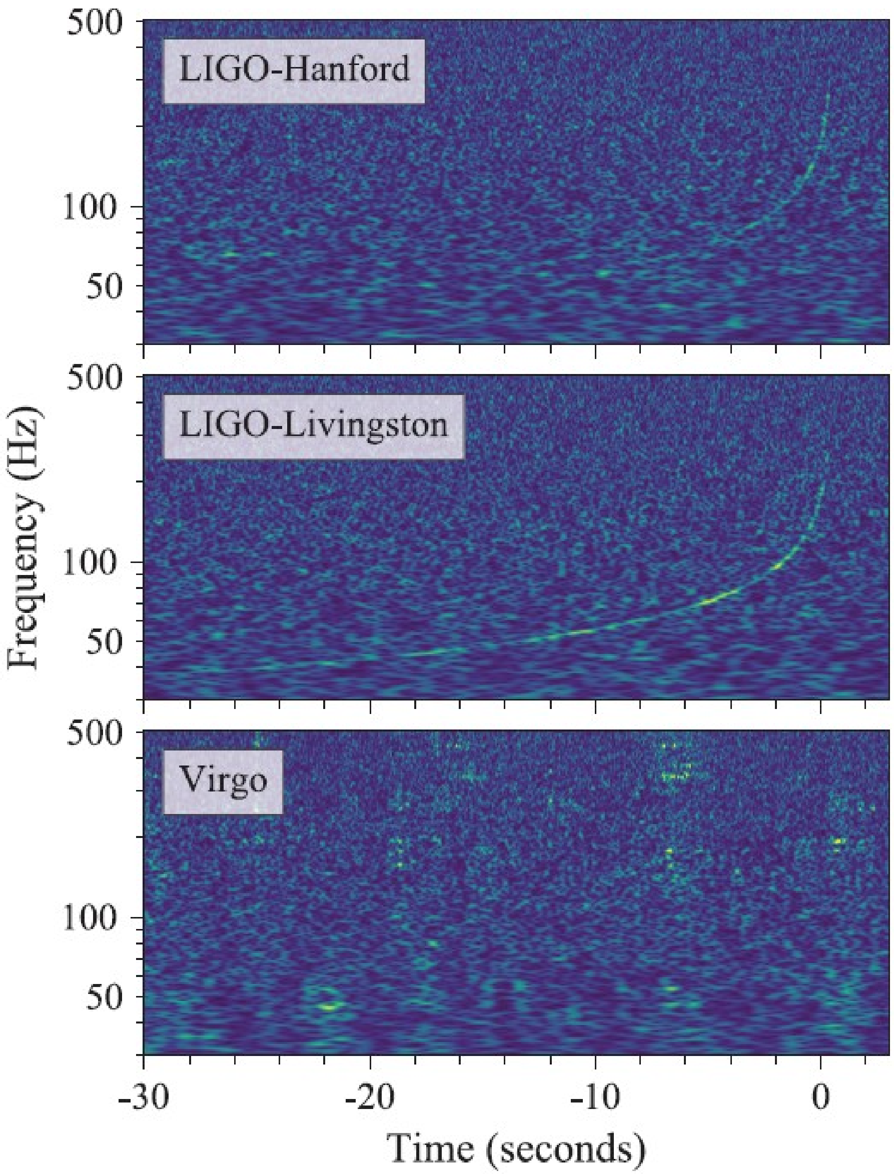

B. P. Abbott et al. PRL 119, 161101 (2017)
(LIGO and Virgo Collaborations)
GW170817: Observation of Gravitational Waves from a Binary Neutron Star Inspiral

tidal (quadrupolar) deformability $\Lambda \sim (R/M)^5$ (the stiffness of a star to the stress caused by its companion's gravity, measures deviation of a gravitational field from that of a pointlike star) $\Lambda < 800$

and

component masses in the range 1.17–1.60 $M_{\odot}$

total mass 2.74 $M_{\odot}$

(spin dependent)

were inferred by matching the observed waveform with a frequency-domain post-Newtonian waveform model.

GW170817 constraints
on the NS Radius and the EOS

E. Annala et al. PRL 120, 172703 (2018)

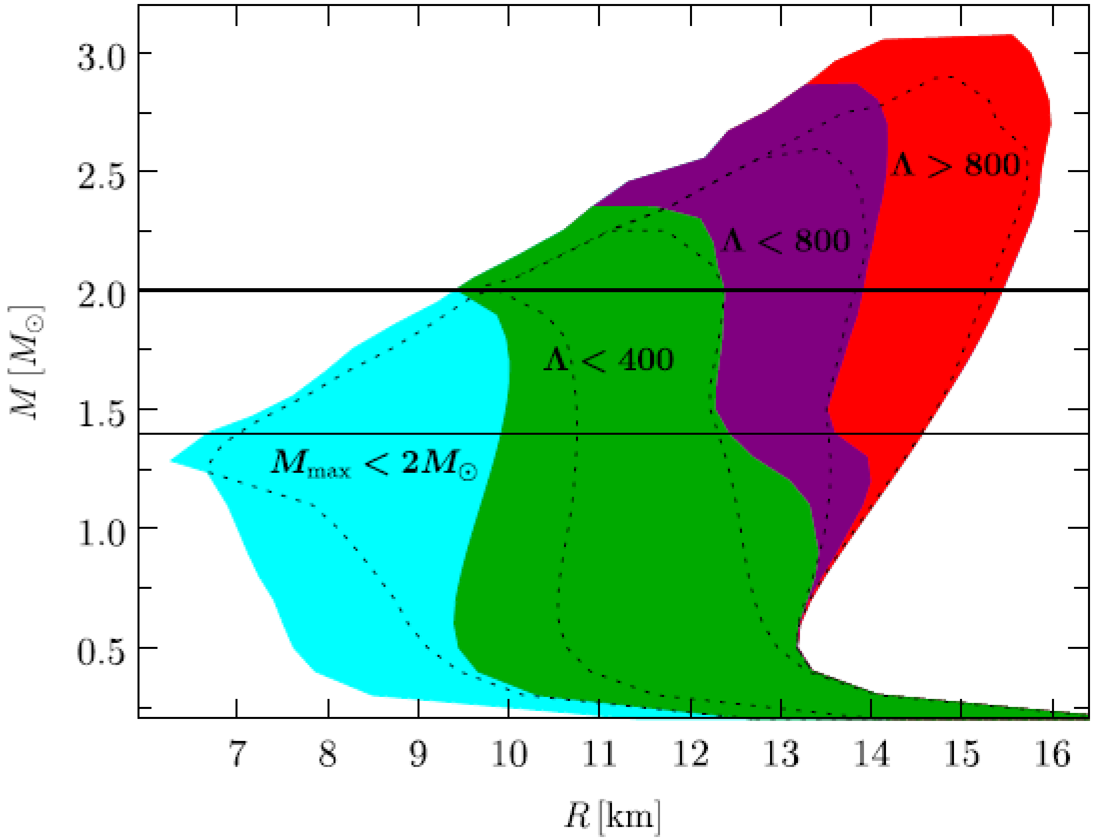

The mass-radius clouds corresponding to our EOSs

$9.9 < R(1.4\ M_{\odot}) < 13.6$ km

$\Lambda(1.4\ M_{\odot}) \geq 120$

J.M. Lattimer, M. Prakash, Physics Reports 621 (2016) 127:

► ~26 < L < ~84 MeV

Compatible with larger NS from qLMXB analyses and thus supporting the stiffer E_{sym}.

GW170817 constraints on the NS Radius and the EOS

C.A. Raithel, F. Özel, & D. Psaltis, AJL 857:L23 (2018)

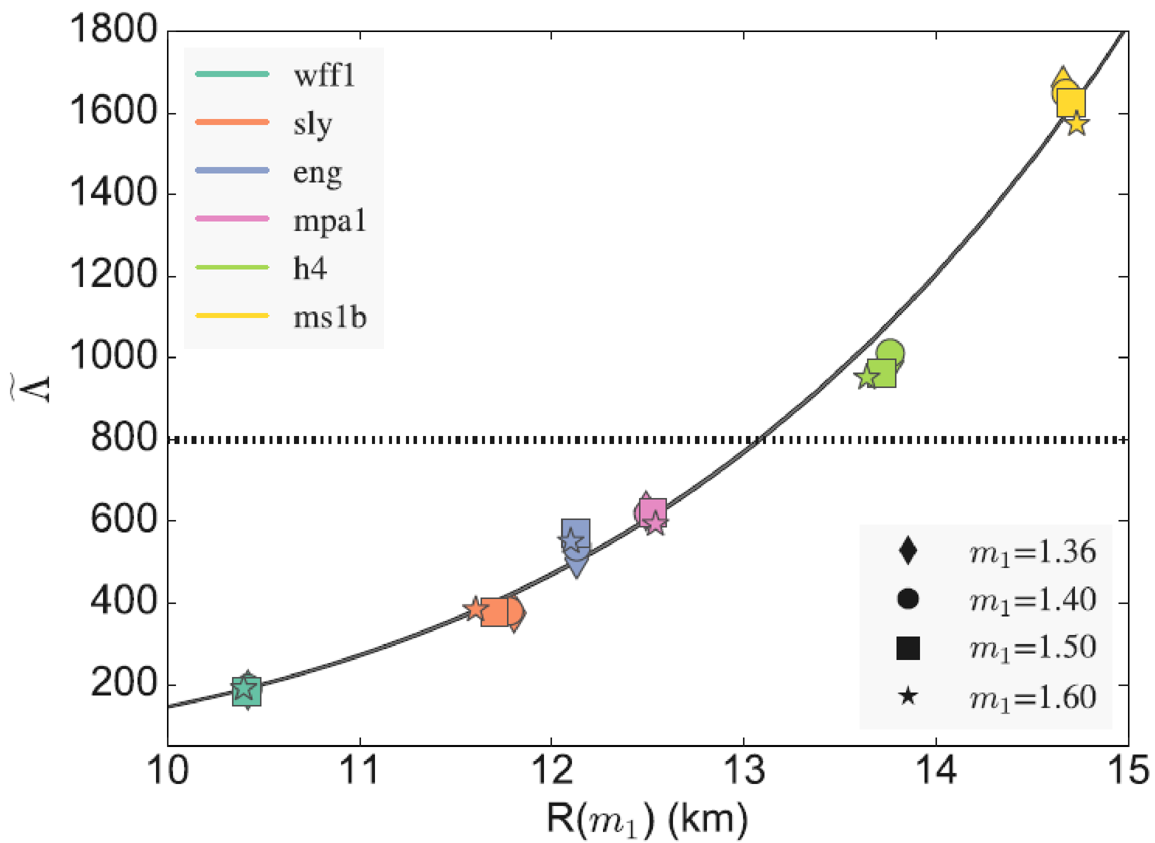

Effective tidal deformability of the binary system as a function of the radius of the primary neutron star, for 6 EoSs.

R(1.4 $M_\odot$) < 13 km
(no lower limit)

Bayesian Inference:
→ most probable Λ = 400
→ most likely radius R_{NS} = 11.7 km

small mass dependence

Supporting rather larger NS

GW170817 constraints on the NS Radius and the EOS

A. Bauswein et al., Astr. J. Lett., 850:L34, 2017

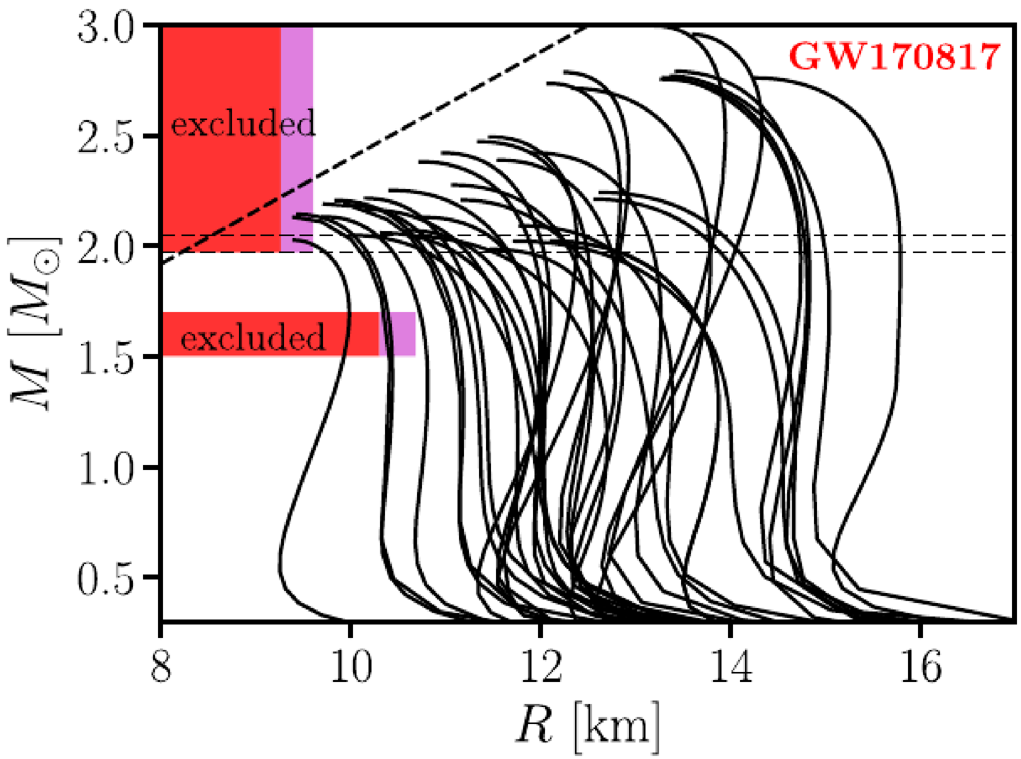

Mass–radius relations of different EoSs with very conservative (red area) and "realistic" (cyan area) constraints of this work for R 1.6 and Rmax. Horizontal lines display the limit by Antoniadis et al. (2013). The dashed line shows the causality limit.

$R(1.6\ M_\odot) > 10.68$ km

Lower limit on the stellar radius of a 1.6 $M_\odot$ neutron star was obtained under the assumption that the merger did not result in a prompt collapse.

GW170817 constraints on the NS Radius and the EOS

F. J. Fattoyev, J. Piekarewicz, and C. J. Horowitz, PRL 120, 172702 (2018)

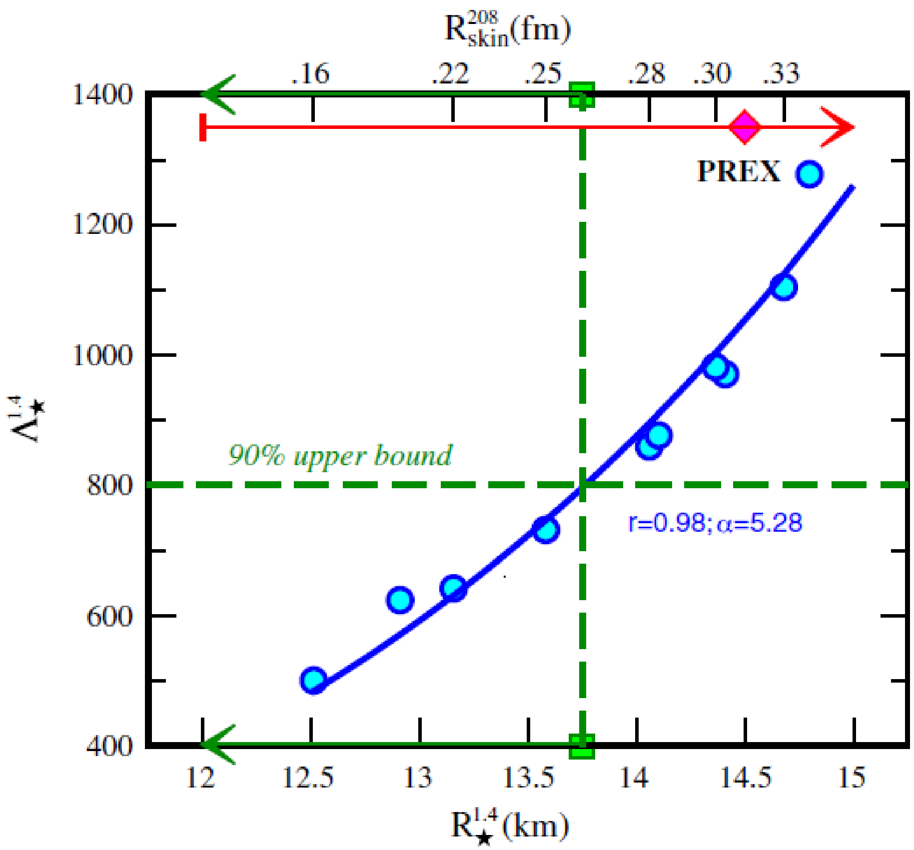

$R(1.4\ M_{\odot}) < 13.76$ km

$\Lambda(1.4\ M_{\odot}) \geq 490$ (PREX lower limit)

$L < 82.5$ MeV (TAMUC-FSUa)

Supporting rather larger NS.
RN and Rskin not quite compatible

The dimensionless tidal polarizability Λ1.4 of a $1.4M_{\odot}$ neutron star as a function of the neutron-skin thickness of 208Pb (upper abscissa) and the radius of a $1.4M_{\odot}$ neutron star (lower abscissa) as predicted by the 10 RMF models.

Squeezing the Symmetry Energy out of Heavy Ion Collisions

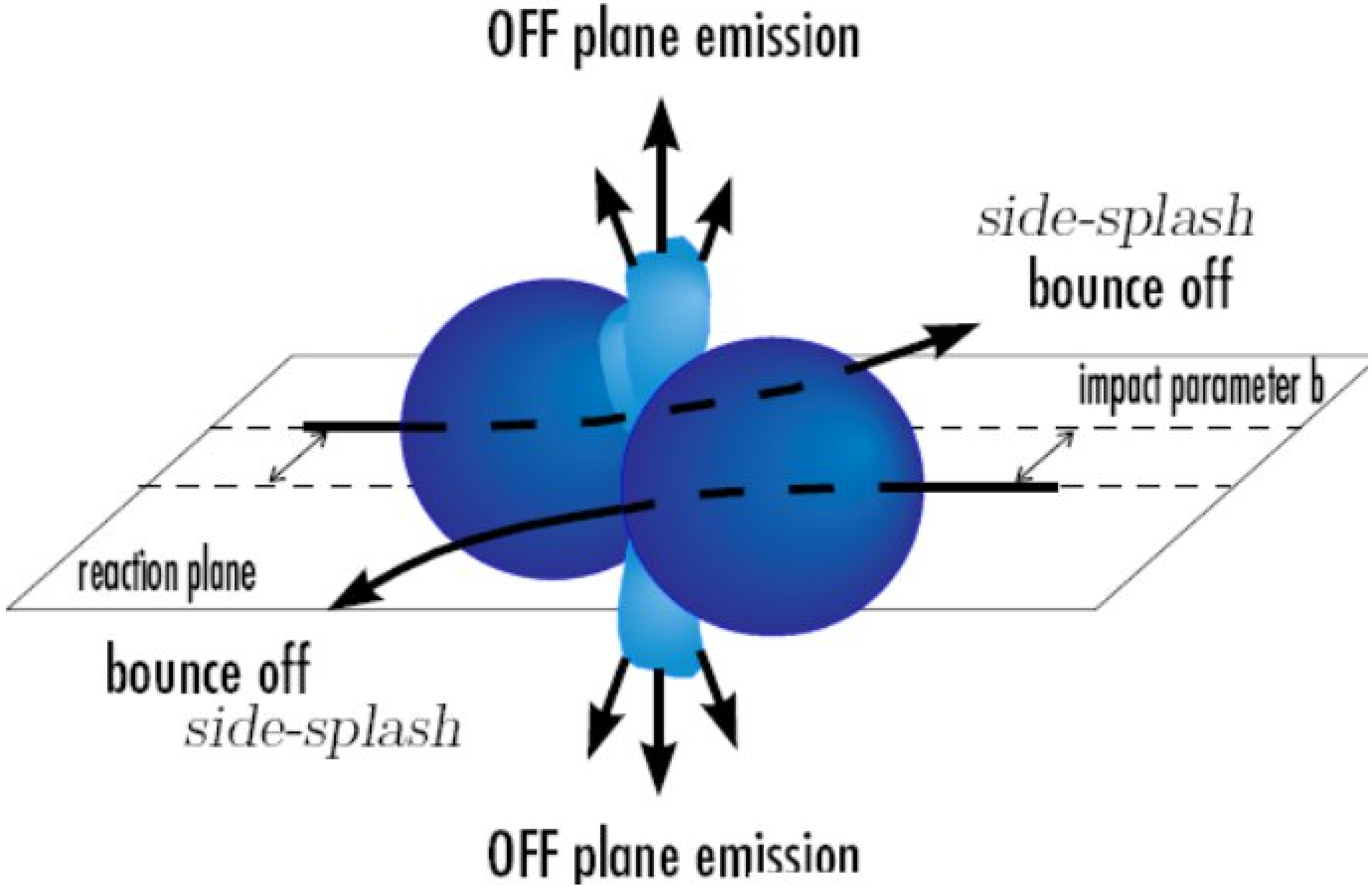

Symmetry energy from low and intermediate energy HI collisions

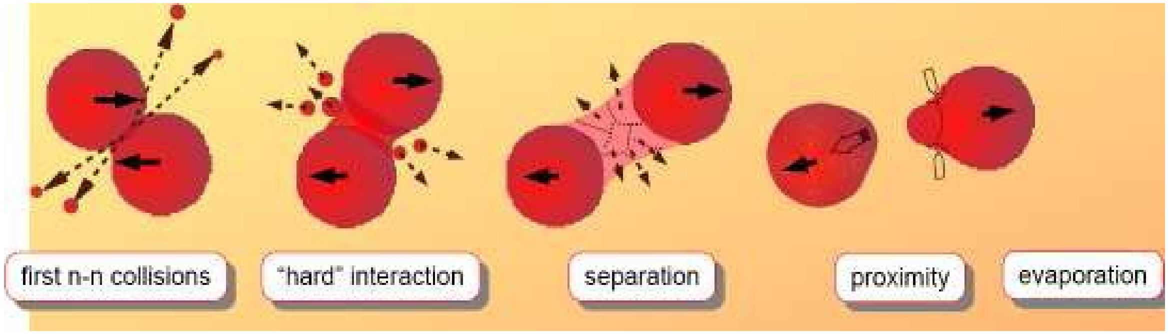

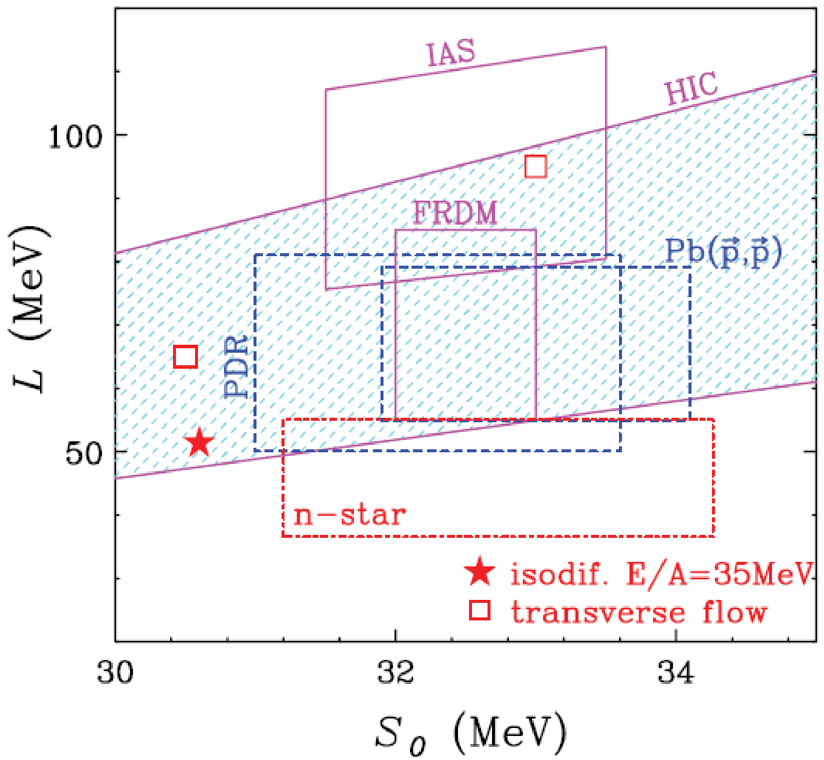

(S_0, L) centered on ~ (32.5, 70) MeV over the range of density between 0.3-1 ρ_0

M.B. Tsang et al., Phys. Rev. C 86 (2012) 015803

HIC - heavy-ion collisions, isospin diffusion, isoscaling, n/p ratios, Tsang et al., 2009, 2012
IAS - isobaric analog states, Danielewicz & Lee 2009, 2012
PDR - pygmy dipole resonances, Klimkiewicz et al. 2007
FRDM – finite-range droplet model, binding energy fits, Moeller et al. 2012
Pb(p,p) – neutron skin thickness from p elastic scattering, Zenihiro et al. 2010

High energy (density) experiments

(1) FOPI/LAND data (GSI 1993/2011)

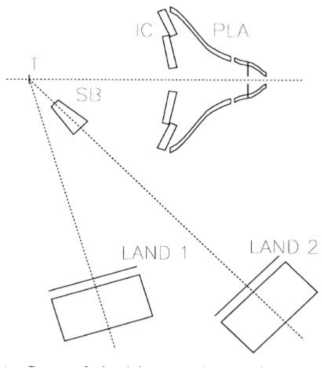

(2) ASY-EOS experiment (GSI 2011)

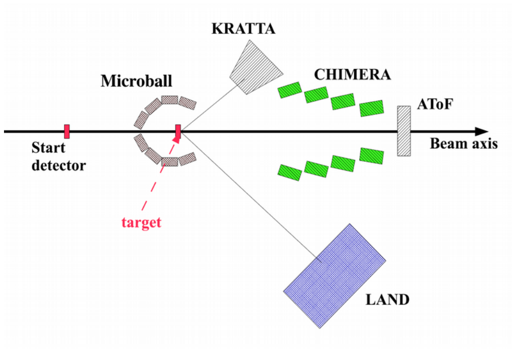

(3) SPiRIT experiment (RIKEN 2016)

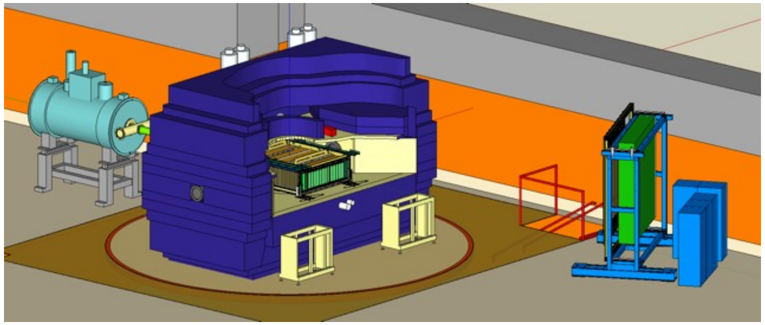

High energy (density) experiments

(1) FOPI/LAND data (GSI 1993/2011)

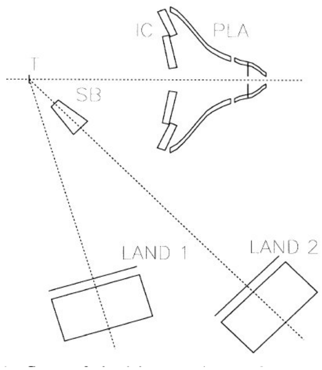

(2) ASY-EOS experiment (GSI 2011)

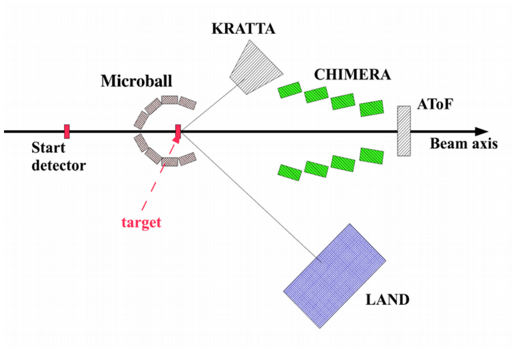

(3) SPiRIT experiment (RIKEN 2016)

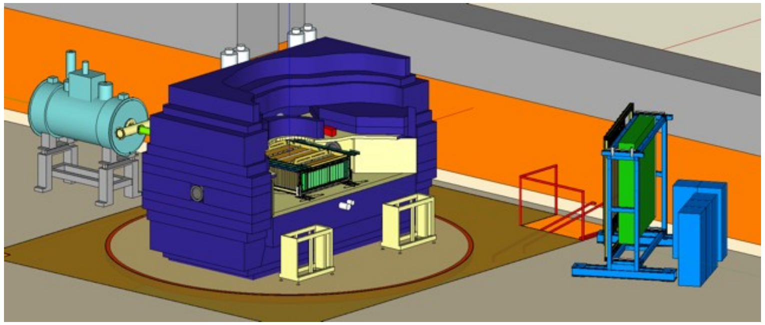

ASY-EOS experimental setup

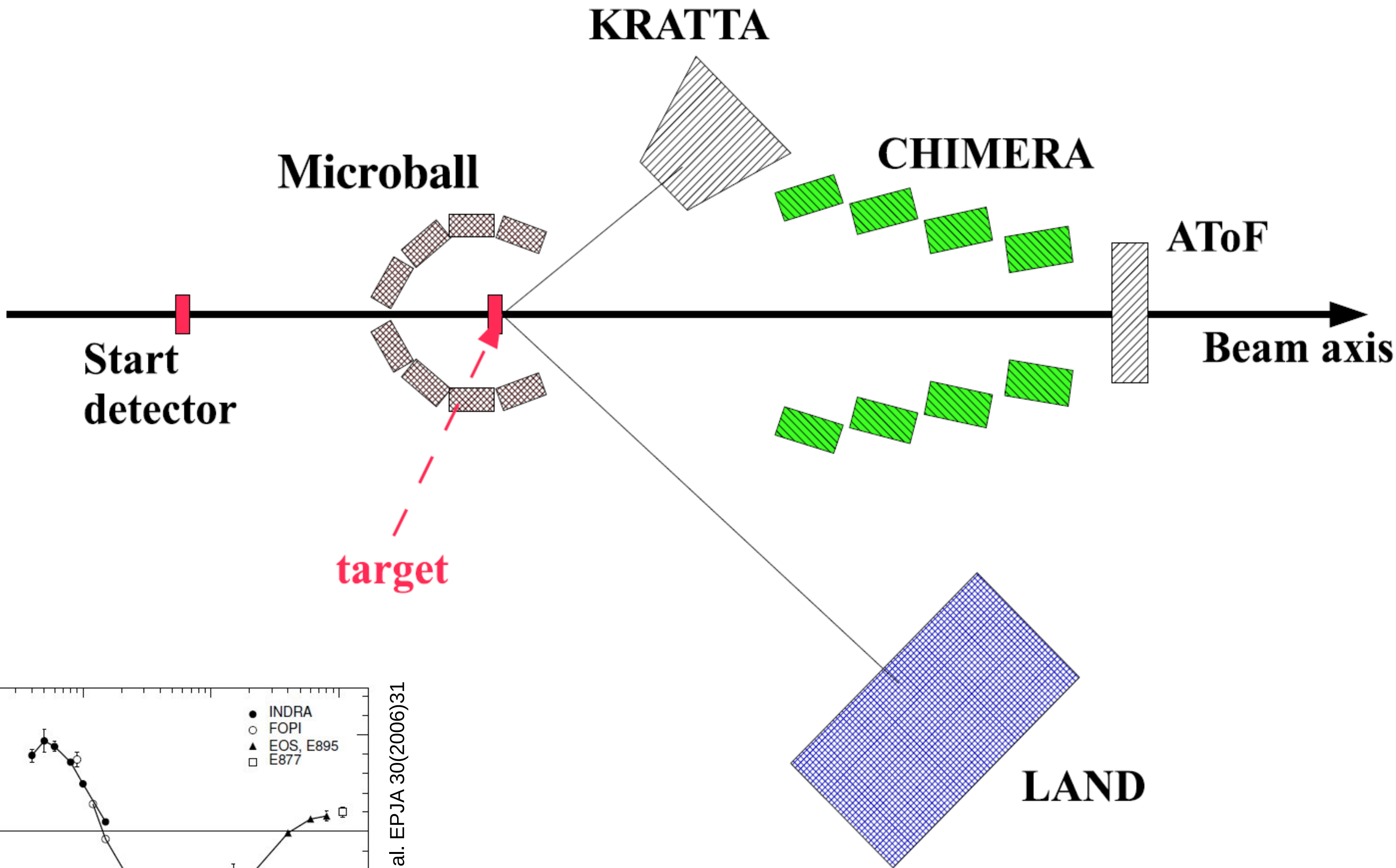

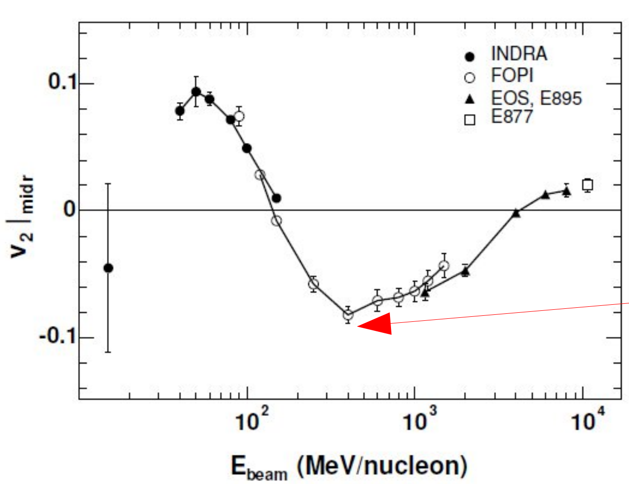

A. Andronic et al. EPJA 30(2006)31

^{197}Au	+	^{197}Au	@ 400 AMeV	$\delta^2 = 0.039$
^{96}Zr	+	^{96}Zr	@ 400 AMeV	$\delta^2 = 0.028$
^{96}Ru	+	^{96}Ru	@ 400 AMeV	$\delta^2 = 0.007$

KRATTA @ GSI (Au+Au at 400 AMeV, 2011)

ASY-EOS Experimental Setup

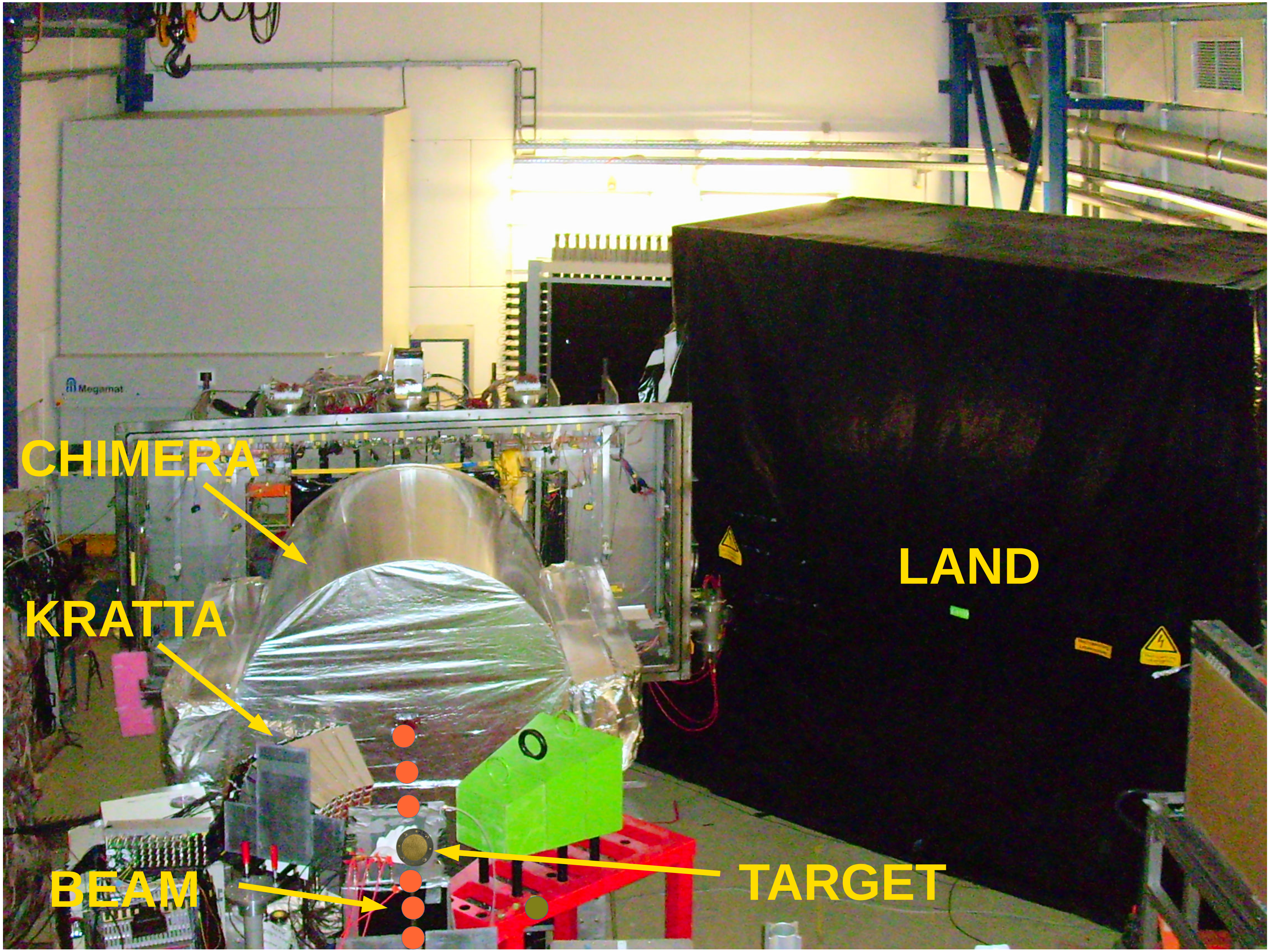

P. Russotto et al., PRC, 94 (2016) 034608

J. Łukasik et al., NIMA 709 (2013) 120

Model assumptions

UrQMD, Q. Li, J.Phys. G 31(2005)1359

„Fermi-gas” parametrization of the symmetry term:

$$E_{sym} = E_{sym}^{pot} + E_{sym}^{kin} = 22\ \mathrm{MeV} \left(\frac{\rho}{\rho_o}\right)^{\gamma} + 12\ \mathrm{MeV} \left(\frac{\rho}{\rho_o}\right)^{2/3}$$

$\gamma = 1.5\,(\mathrm{STIFF})$

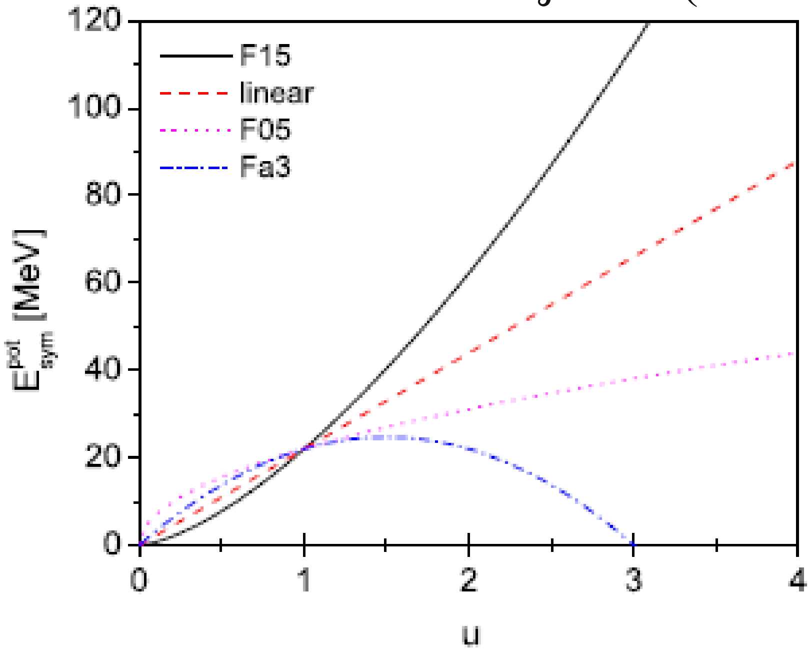

$\gamma = 0.5\,(\mathrm{SOFT})$

Flow analysis (v_1, v_2)

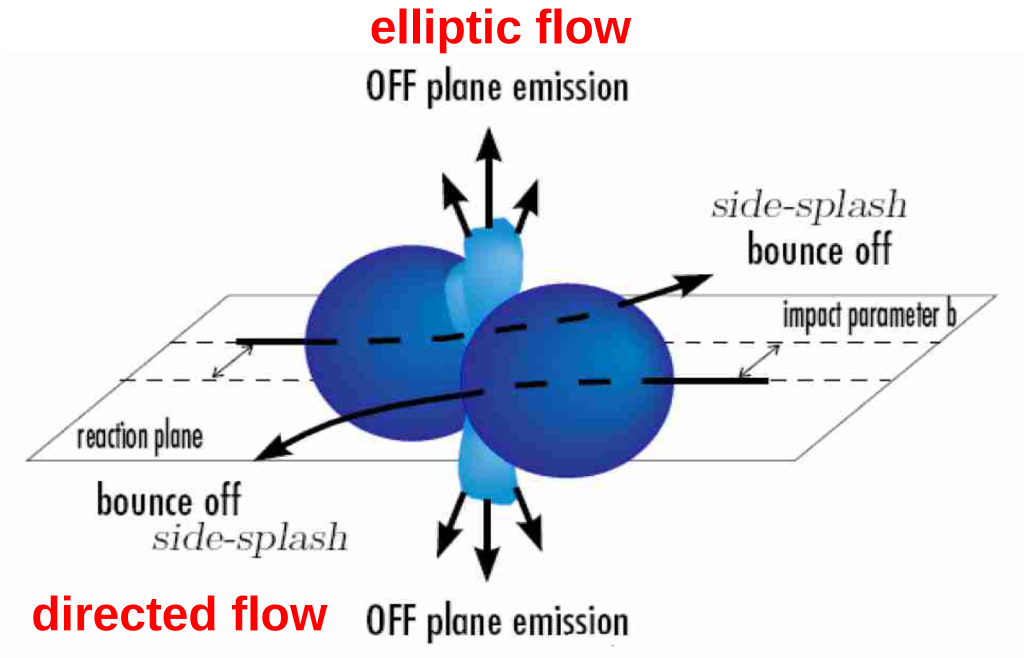

Fourier decomposition of **azimuthal distributions** with respect to the **reaction plane** (φ_R):

$$\frac{dN}{d(\phi-\phi_R)} = \frac{N_0}{2\pi}\left(1+2\sum_{n\geq 1} v_n \cos n(\phi-\phi_R)\right)$$

directed flow: $v_1 \equiv \langle \cos(\phi-\phi_R)\rangle$

elliptic flow: $v_2 \equiv \langle \cos 2(\phi-\phi_R)\rangle$

$v_n = v_n(b, Z, A, y, p^T)$

W. Trautmann et al., 2011

Au+Au @ 400 AMeV

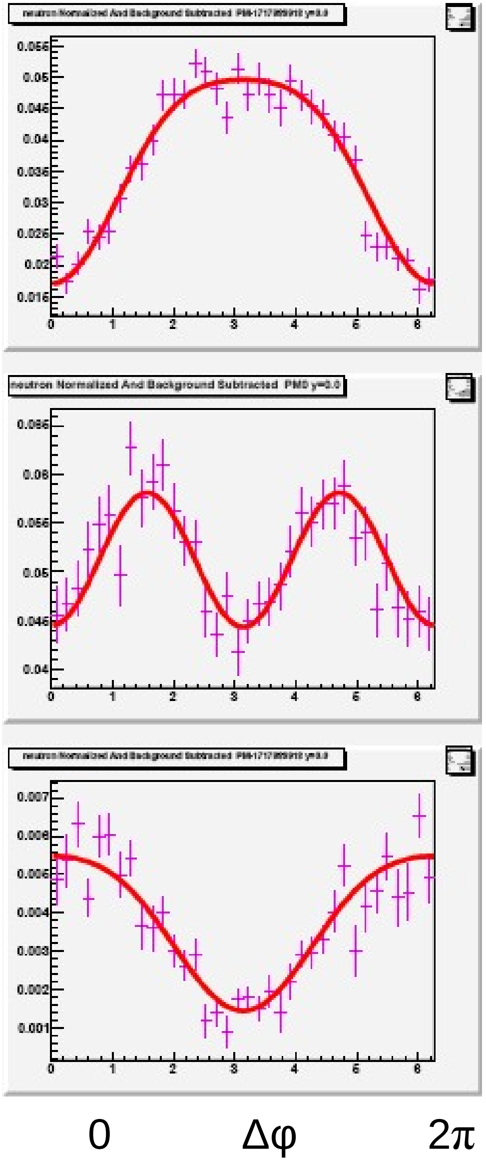

Target rapidity (strong directed flow)

Mid-rapidity (strong elliptic flow- squeeze-out)

Projectile rapidity (strong directed flow)

FOPI-LAND LAND@ASY-EOS

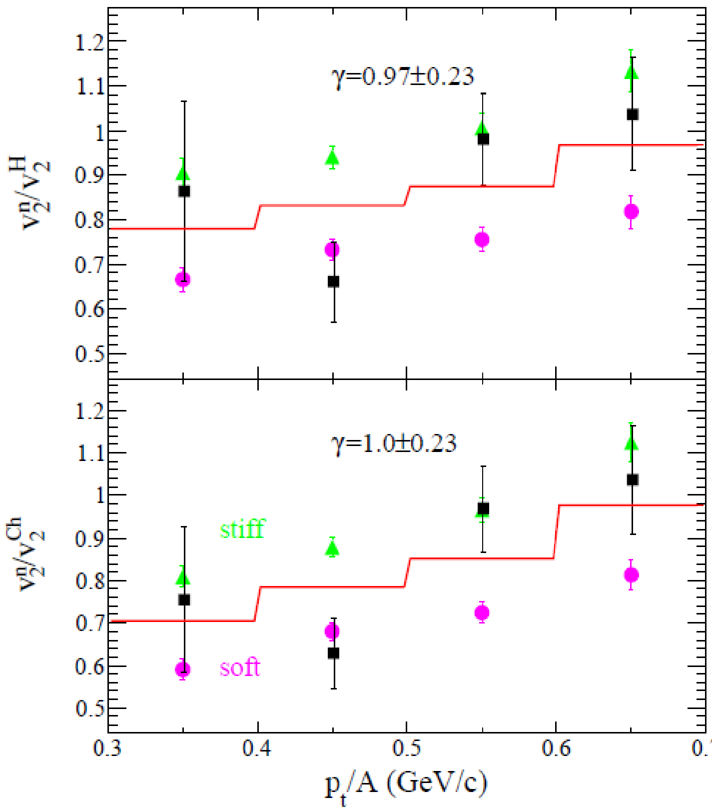

FIG. 14: (Color online) FOPI-LAND data: Elliptic flow ratio of neutrons over all hydrogen isotopes (top) and of neutrons over all charged particles (bottom) for moderately central ($b < 7.5$ fm) collisions of ^{197}Au+^{197}Au at 400 MeV/nucleon, as a function of the transverse momentum per nucleon p_t/A. The black symbols represent the experimental data. The UrQMD predictions for stiff ($\gamma = 1.5$, green symbols) and soft ($\gamma = 0.5$, purple symbols) are shown. The red line in each panel is the result of a linear interpolation between the predictions; the obtained gamma values and their uncertainties are indicated.

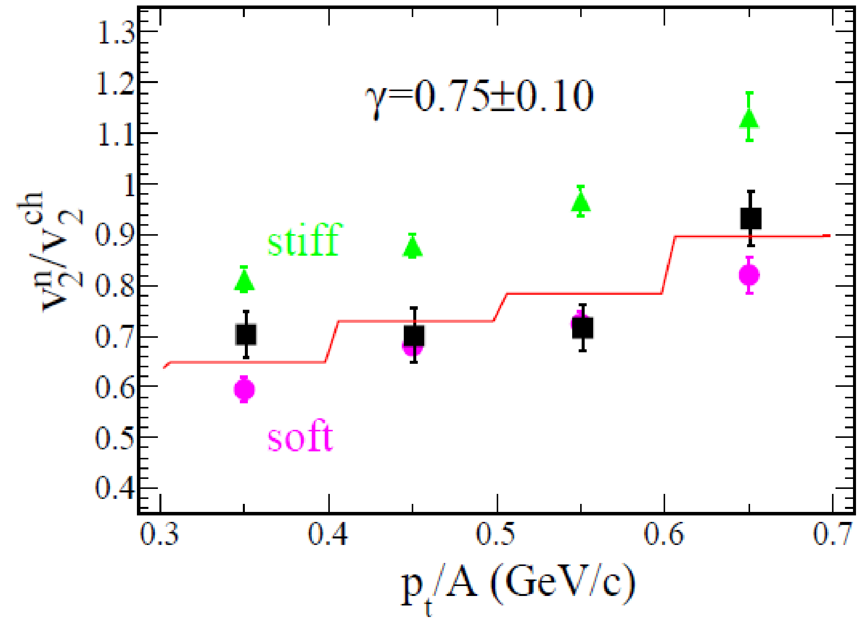

FIG. 15: (Color online) Elliptic flow ratio of neutrons and charged particles for moderately central ($b < 7.5$ fm) collisions of ^{197}Au+^{197}Au at 400 MeV/nucleon as a function of the transverse momentum per nucleon p_t/A, evaluated with a fraction of 80% for the second step of timing corrections (see Sec. IV A). The full squares represent the experimental data, the triangles and dots represent the UrQMD predictions for stiff ($\gamma = 1.5$) and soft ($\gamma = 0.5$) power-law exponents of the potential term. The full line is the result of a linear interpolation between the predictions, leading to the indicated $\gamma = 0.75 \pm 0.10$.

P. Russotto et al., Phys. Rev. C 94 (2016) 034608.

LAND@ASY-EOS

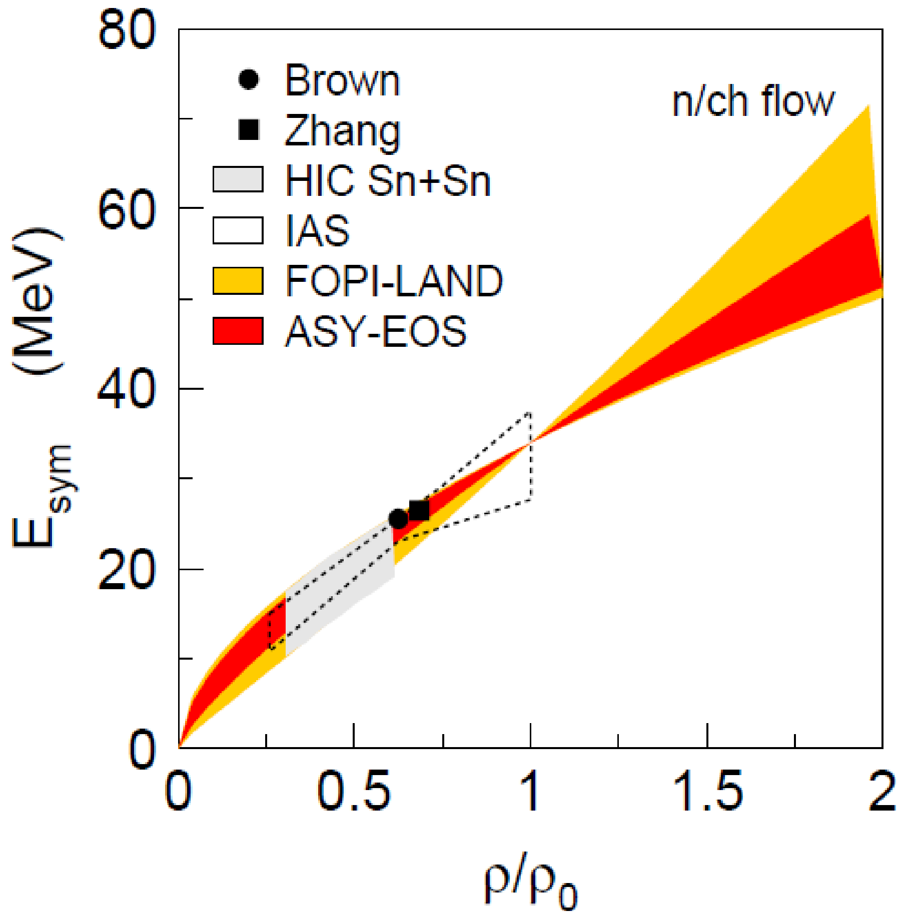

FIG. 19: (Color online) Constraints deduced for the density dependence of the symmetry energy from the present data in comparison with the FOPI-LAND result of Ref. [5] as a function of the reduced density ρ/ρ_0. For reference, the low-density results of Refs. [66–69] as presented in Ref. [70] are included.

$\gamma = 0.72 \pm 0.19$

$L = 72 \pm 13$ MeV

P. Russotto et al., Phys. Rev. C 94 (2016) 034608.

LAND@ASY-EOS

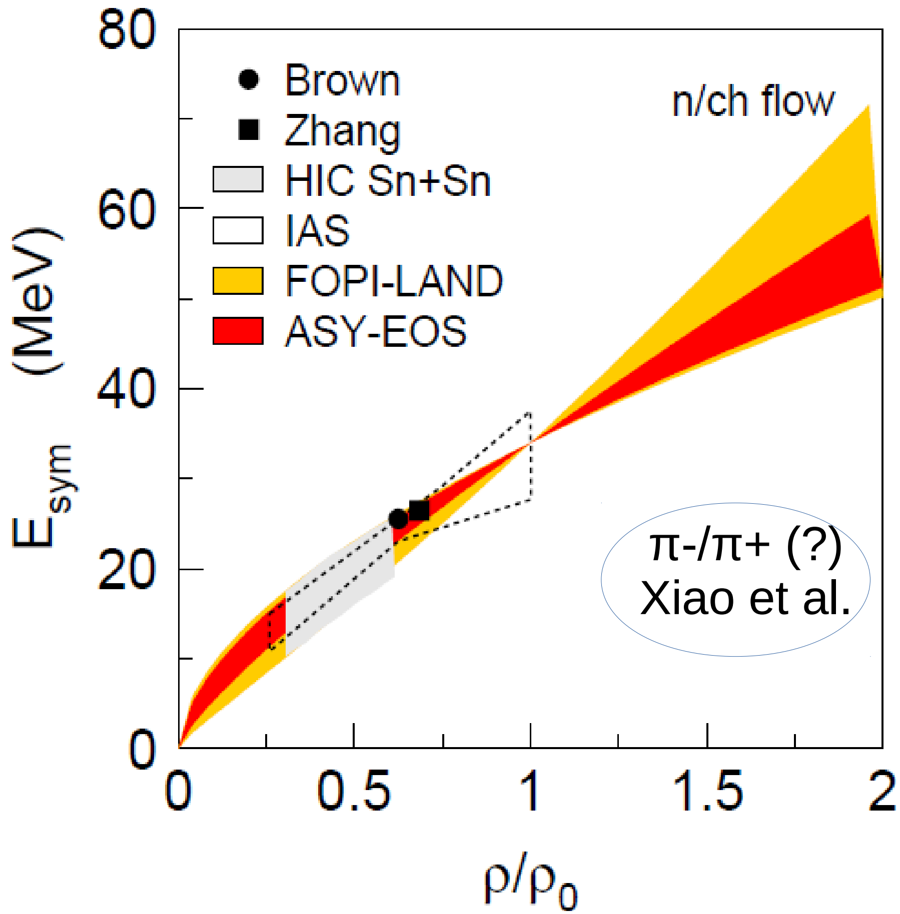

FIG. 19: (Color online) Constraints deduced for the density dependence of the symmetry energy from the present data in comparison with the FOPI-LAND result of Ref. [5] as a function of the reduced density ρ/ρ_0. For reference, the low-density results of Refs. [66–69] as presented in Ref. [70] are included.

$\gamma = 0.72 \pm 0.19$

$L = 72 \pm 13$ MeV

P. Russotto et al., Phys. Rev. C 94 (2016) 034608.

A well known figure

B.-A. Li, Nucl. Phys. News, 27 (2017) 7

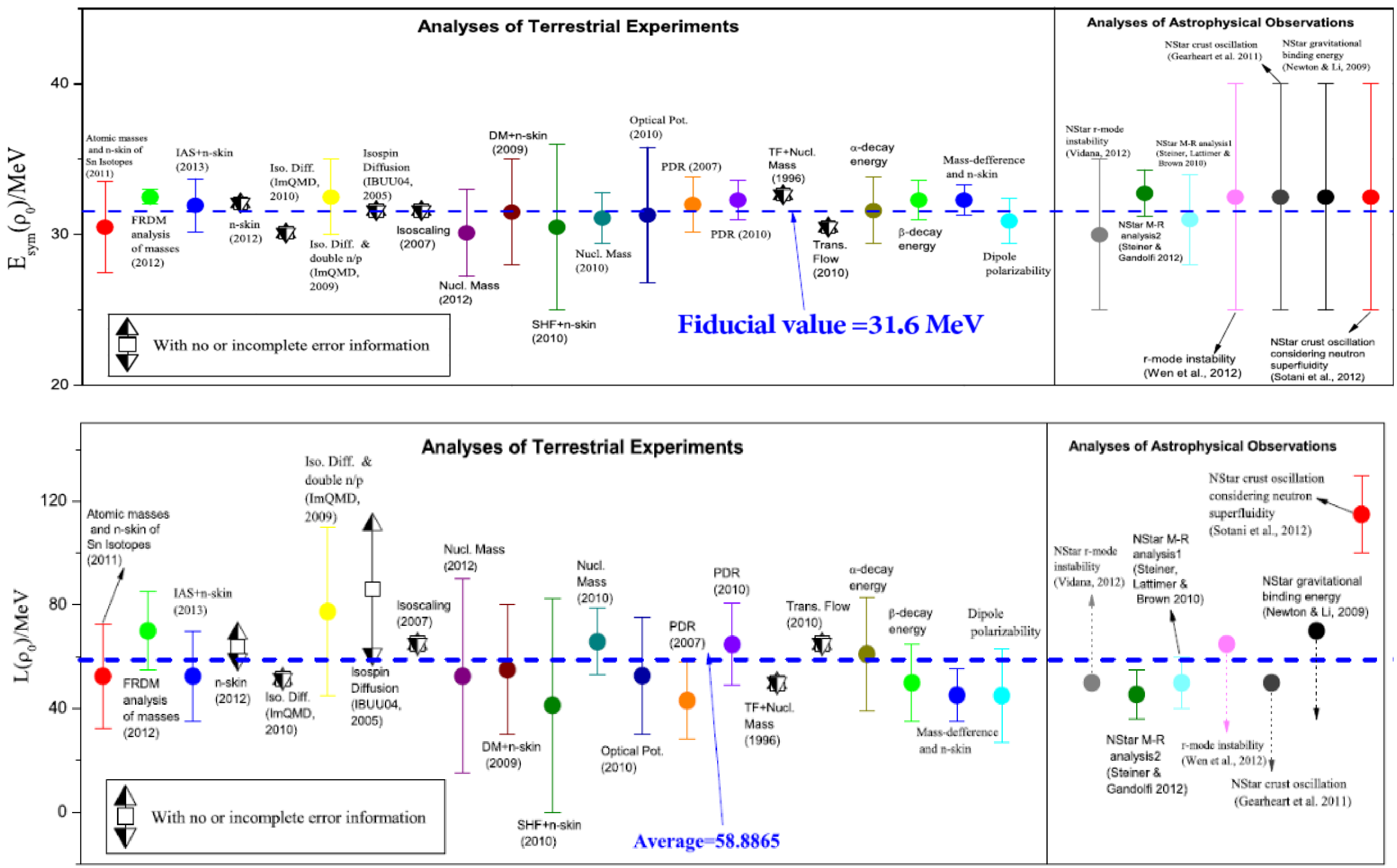

Symmetry energy parameters at ρ_0 from 28 analyses of terrestrial nuclear laboratory experiments and astrophysical observations.

B.-A. Li, Nucl. Phys. News, 27 (2017) 7
P. Russotto et al. Phys. Lett. B 697 (2011) 471; Phys. Rev. C 94 (2016) 034608
Y. Wang et al, Phys. Rev. C 89 (2014) 044603
M.D. Cozma et al., Phys. Rev C 88 (2013) 044912
M.D. Cozma, Eur. Phys. J. A 54 (2018) 40

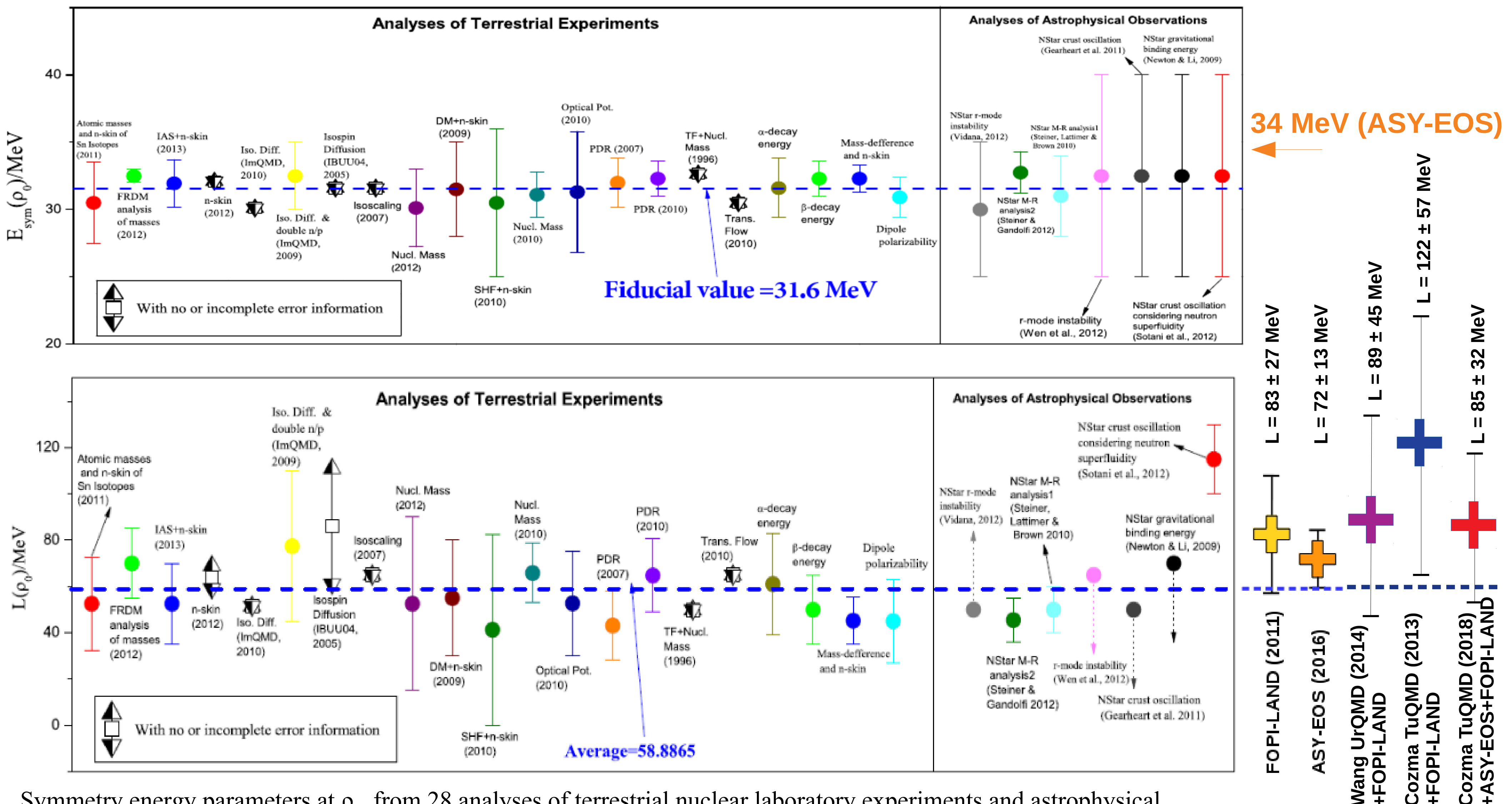

Symmetry energy parameters at ρ_0 from 28 analyses of terrestrial nuclear laboratory experiments and astrophysical observations. Additional five symbols on the right side represent the results of the FOPI-LAND (yellow) and of the ASY-EOS (orange) high energy experiments, the violet cross shows the Skyrme-UrQMD result for the FOPI-LAND data and the blue and red crosses show the TuQMD result for the FOPI-LAND and the FOPI-LAND and ASY-EOS data, respectively.

B.-A. Li, Nucl. Phys. News, 27 (2017) 7
P. Russotto et al. Phys. Lett. B 697 (2011) 471; Phys. Rev. C 94 (2016) 034608
Y. Wang et al, Phys. Rev. C 89 (2014) 044603
M.D. Cozma et al., Phys. Rev C 88 (2013) 044912
M.D. Cozma, Eur. Phys. J. A 54 (2018) 40
F. J. Fattoyev et al., PRL 120, 172702 (2018) (Λ<800, L < 82.5 MeV)

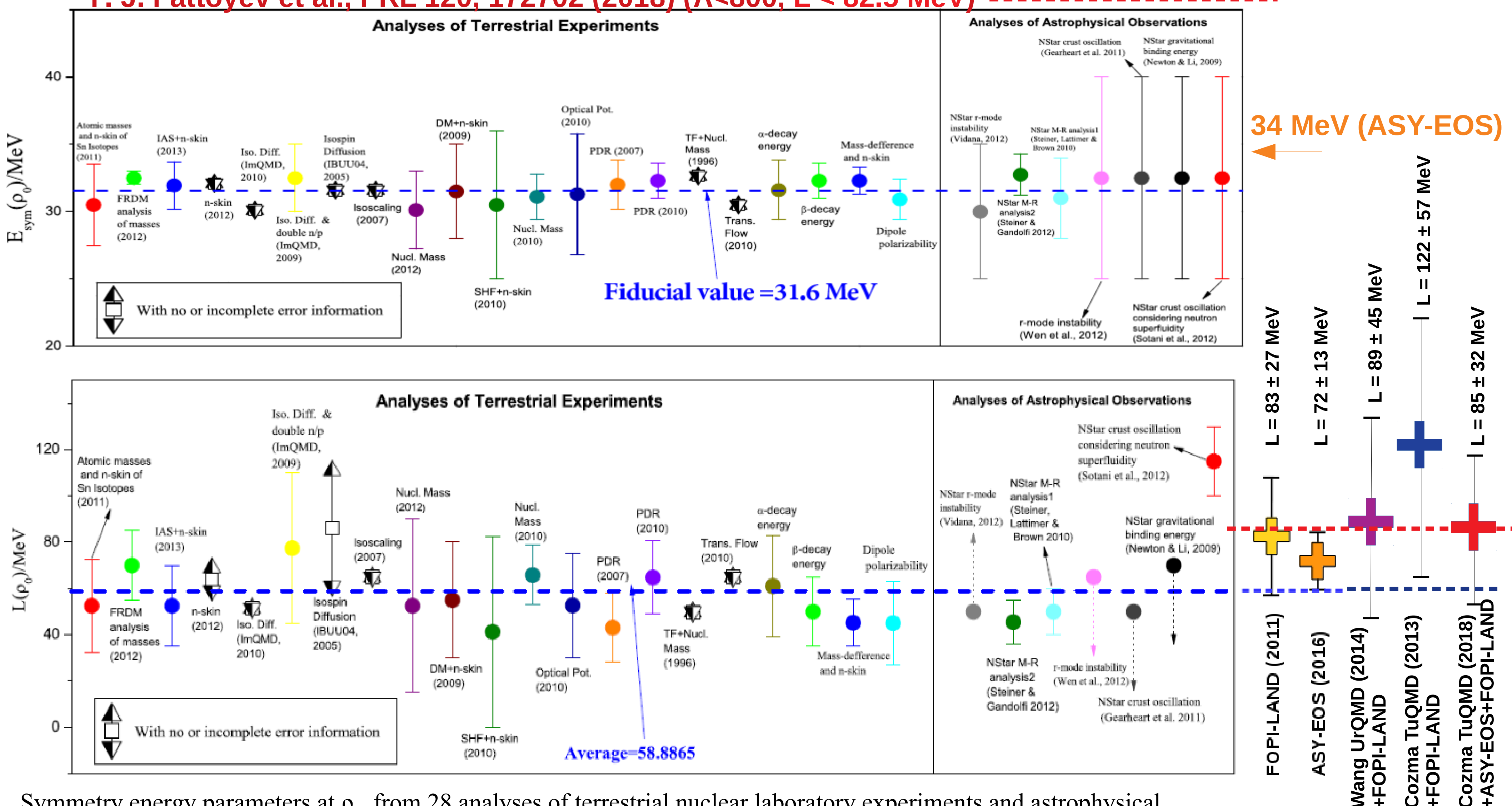

Symmetry energy parameters at ρ_0 from 28 analyses of terrestrial nuclear laboratory experiments and astrophysical observations. Additional five symbols on the right side represent the results of the FOPI-LAND (yellow) and of the ASY-EOS (orange) high energy experiments, the violet cross shows the Skyrme-UrQMD result for the FOPI-LAND data and the blue and red crosses show the TuQMD result for the FOPI-LAND and the FOPI-LAND and ASY-EOS data, respectively.

QMC predictions

S. Gandolfi et al., Phys. Rev. C 85, 032801(R) (2012)

❶

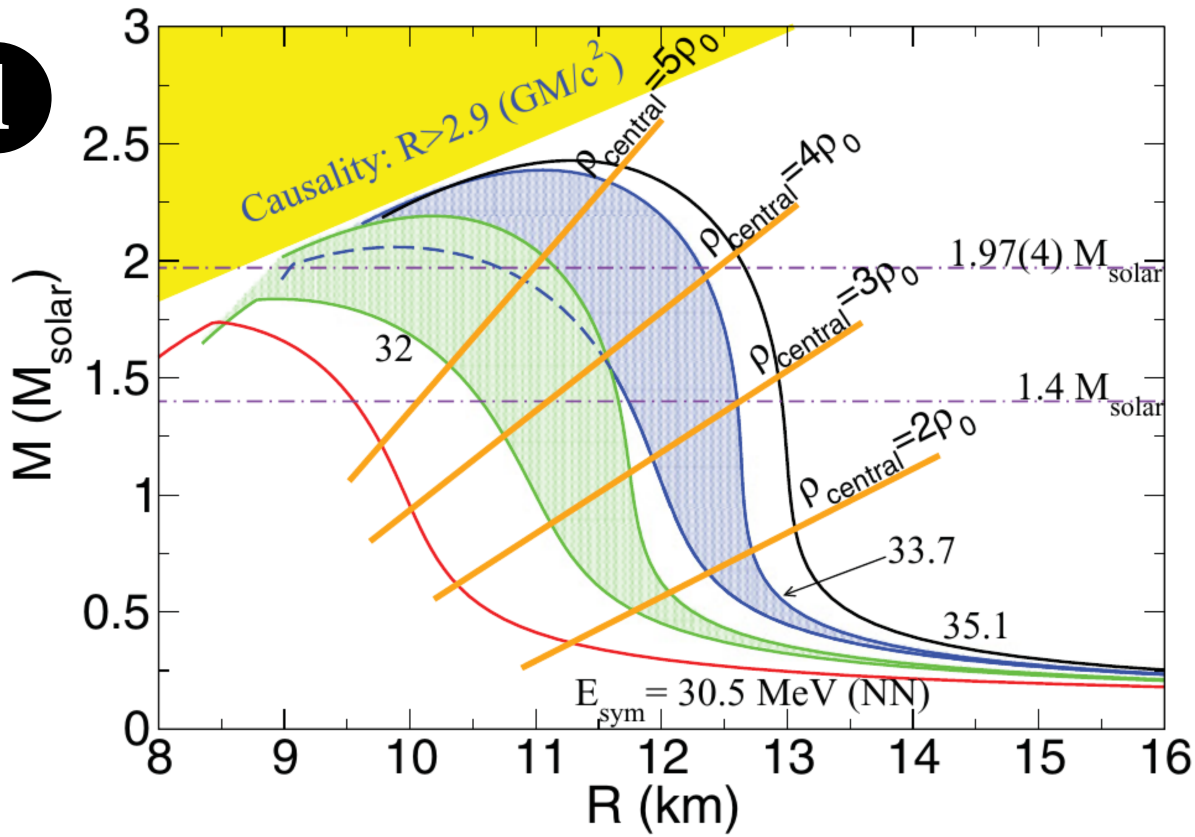

FIG. 2. (Color online) Mass-radius relation for the EoS with three-neutron interactions corresponding to the bands for different $E_{\rm sym}$ shown in Fig. 1. The intersections with the orange lines roughly indicate central densities realized in these stars.

❷

"The uncertainty in the measured symmetry energy of ±2 MeV leads to an uncertainty of about 3 km for the radius."

❶ → measure the symmetry energy at high densities (energies) to probe the EOS in the core of NS

❷ → measure the symmetry energy as precise as possible to provide constraints relevant for astrophysics.

densities probed in HIC

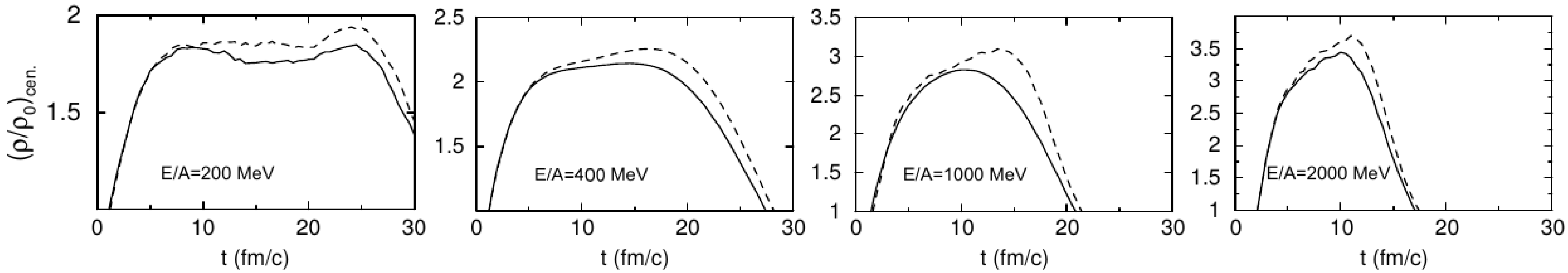

Figure 3: Evolution of the central baryon density in ^{132}Sn+^{124}Sn collisions at beam energies from 200 to 2000 MeV/nucleon for b = 1 fm, as predicted by the hadronic transport model of [31].

adapted from B.-A. Li, Nucl. Phys. A 708 (2002) 365.

UrQMD predictions

flow ratios

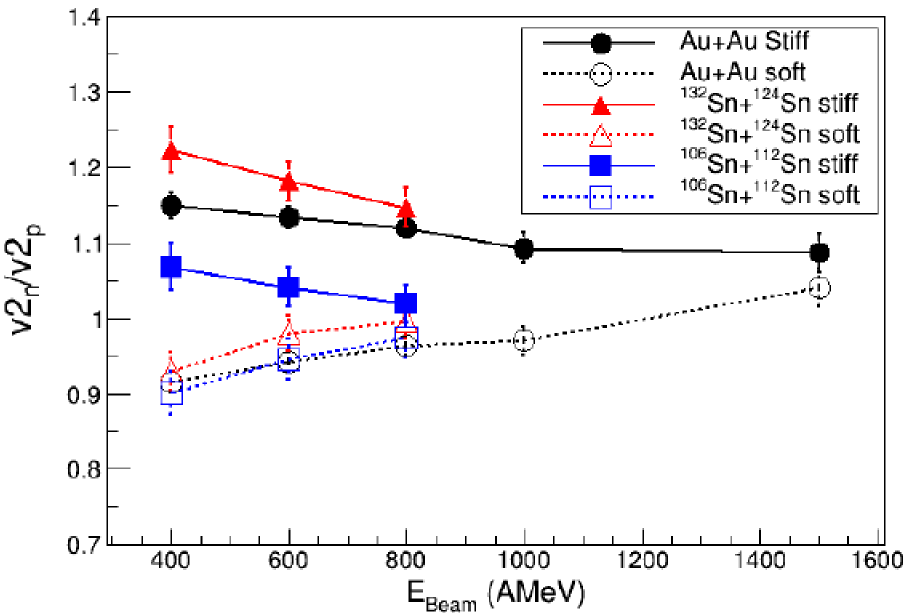

sensitivity

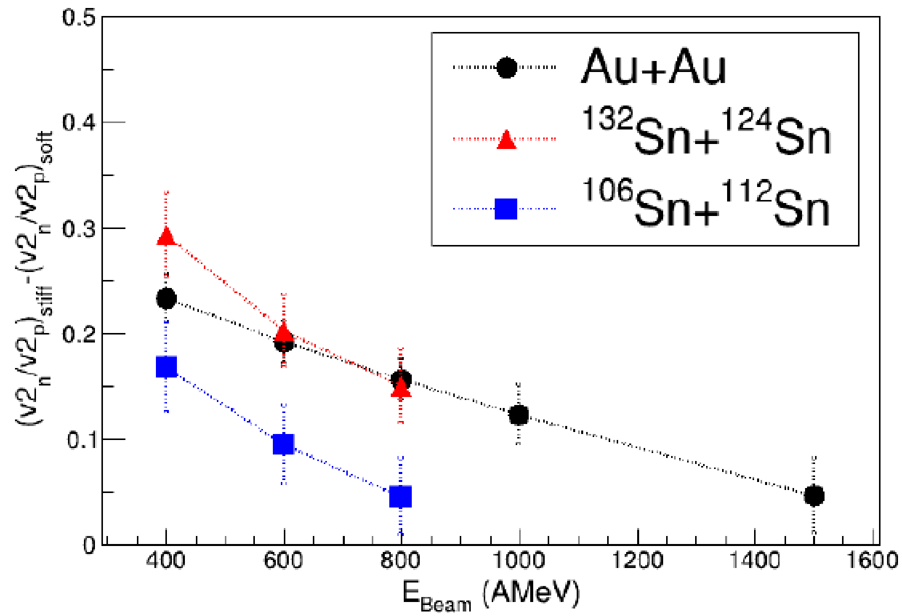

Figure 4: Left panel: Excitation functions of neutron-to-proton elliptic flow ratios, $v2_n/v2_p$, at mid-rapidity for semi-central Au+Au, ^{132}Sn+^{124}Sn, and ^{106}Sn+^{112}Sn collisions, as predicted by the UrQMD model for stiff and soft $E_{sym}(\rho)$. Right panel: differences between the stiff and soft results.

P. Russotto

ASY-EOS II @ FAIR (202?)

Determination of the density dependence of the EOS at supra-saturation densities

Symmetric and asymmetric systems
^{108}Sn, ^{132}Sn, ^{197}Au @ 0.4, 1, 1.2 AGeV

Observables:
ratios: n/p, t/^{3}He, π^{-}/π^{+}(?)
flow: n, p, t, ^{3}He

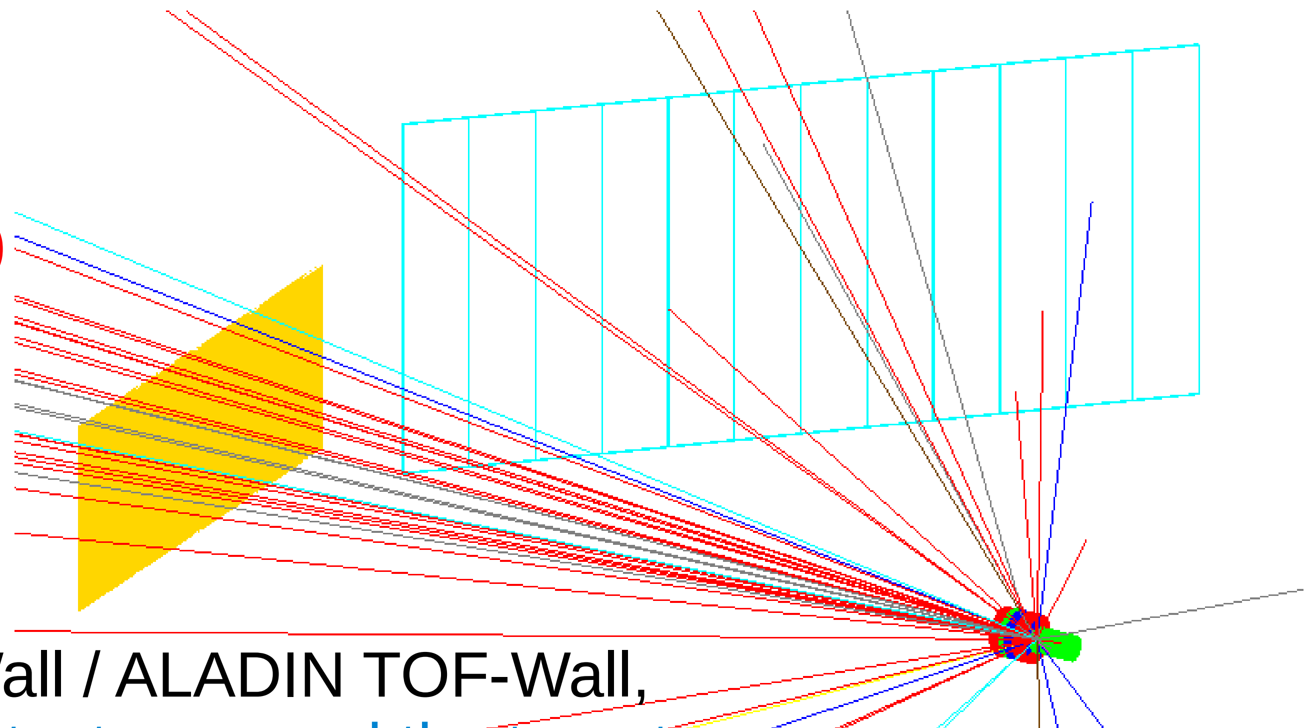

Main detectors:
NeuLAND, FOPI PlasticWall / ALADIN TOF-Wall,
Trigger/Reaction Plane detector around the target

Trigger/Reaction Plane detector around the target

requirements:

- should cover angles > 30^o,
- high segmentation in azimuthal angle,
- high geometrical efficiency,
- low multihit probability,
- fast timing

Trigger/Reaction Plane detector around the target:

- 5 rings of 4x4 mm^2 fast scintillating fibers (e.g. BCF-20) read out by SiPMs
- covers angles from 30^o to 165^o,
- segmentation assures more or less uniform count rates for Au+Au at 1 AGeV,
- geometrical efficiency ~87%
- ~10% of charged particles involved in multihits,
- ~5% multihit probability
- sufficiently large for radioactive beams
- sufficiently small and lightweight not to disturb neutrons
- min radius - 6 cm,
- max radius - 12 cm
- length 43 cm
- 160 segments in forward rings
- 96 segments in backward ring
- 736 channels

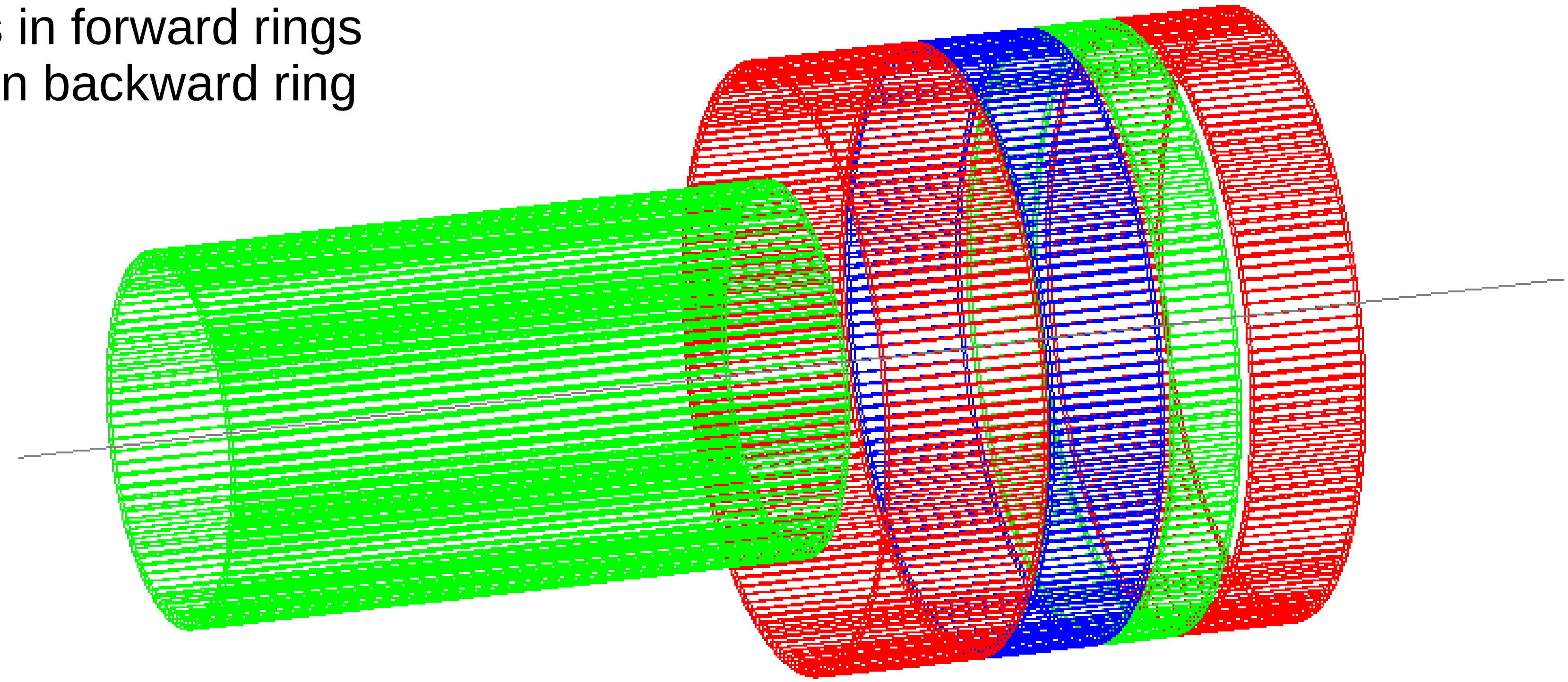

UrQMD + clustering: Au+Au 1000 AMeV, 0-10 fm, 200 fm/c

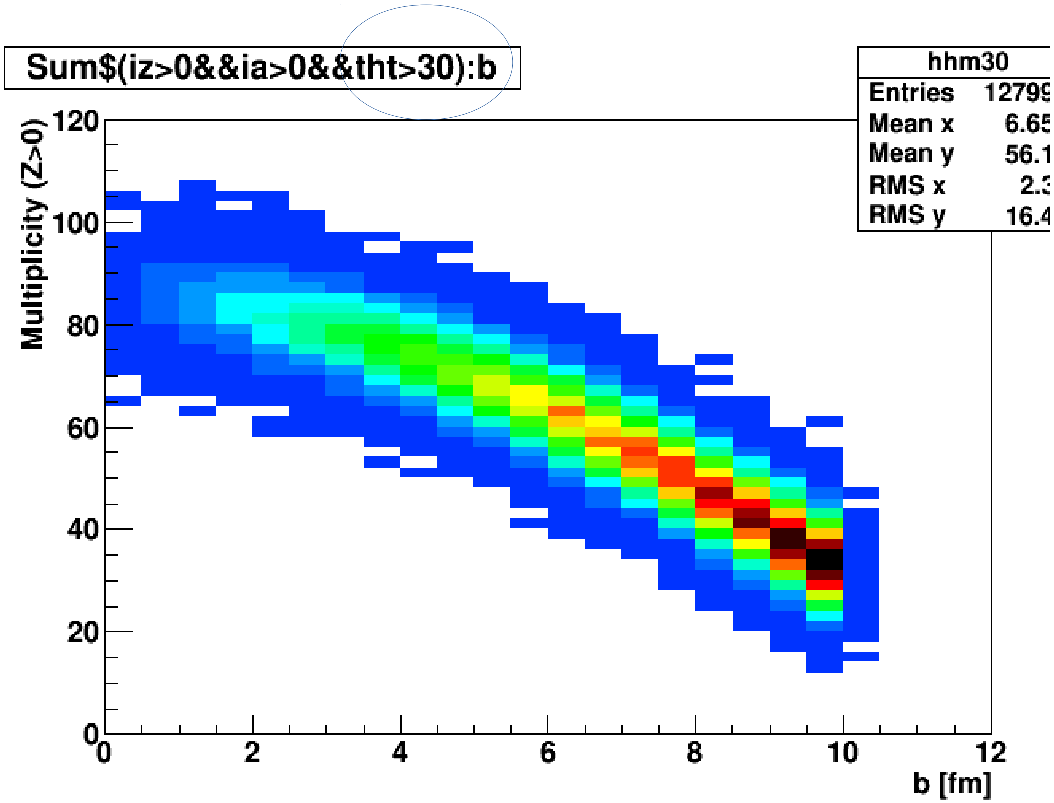

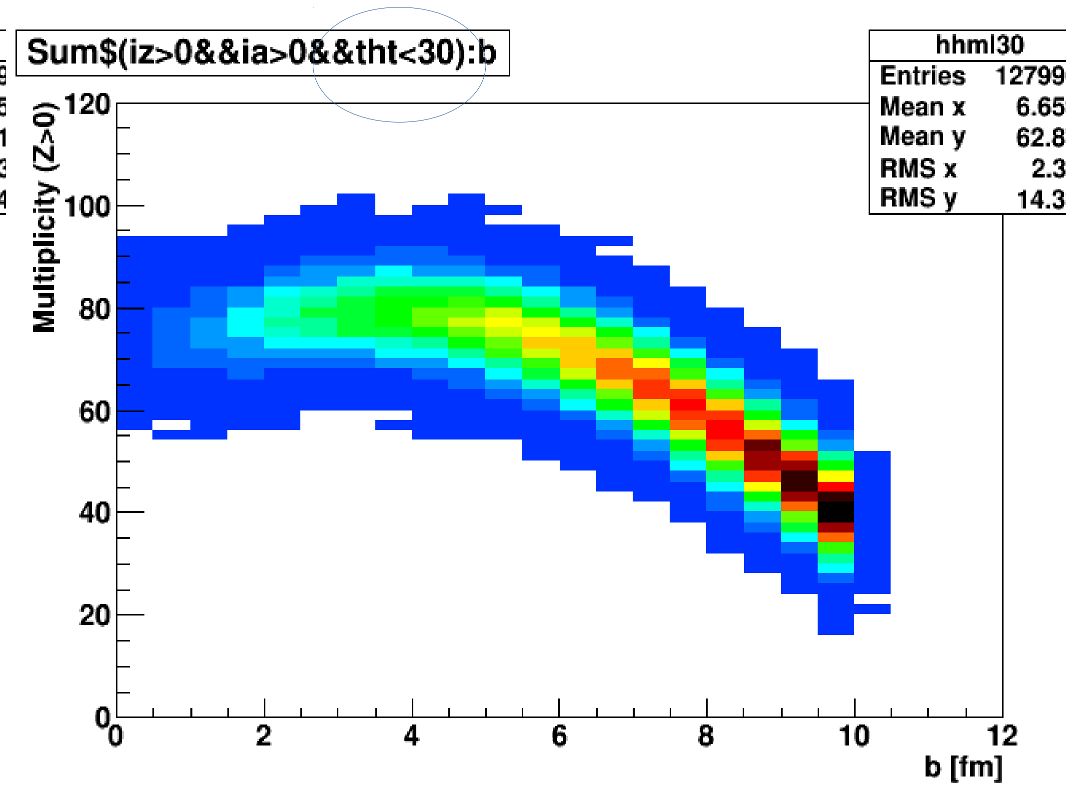

better correlation

hits/segment

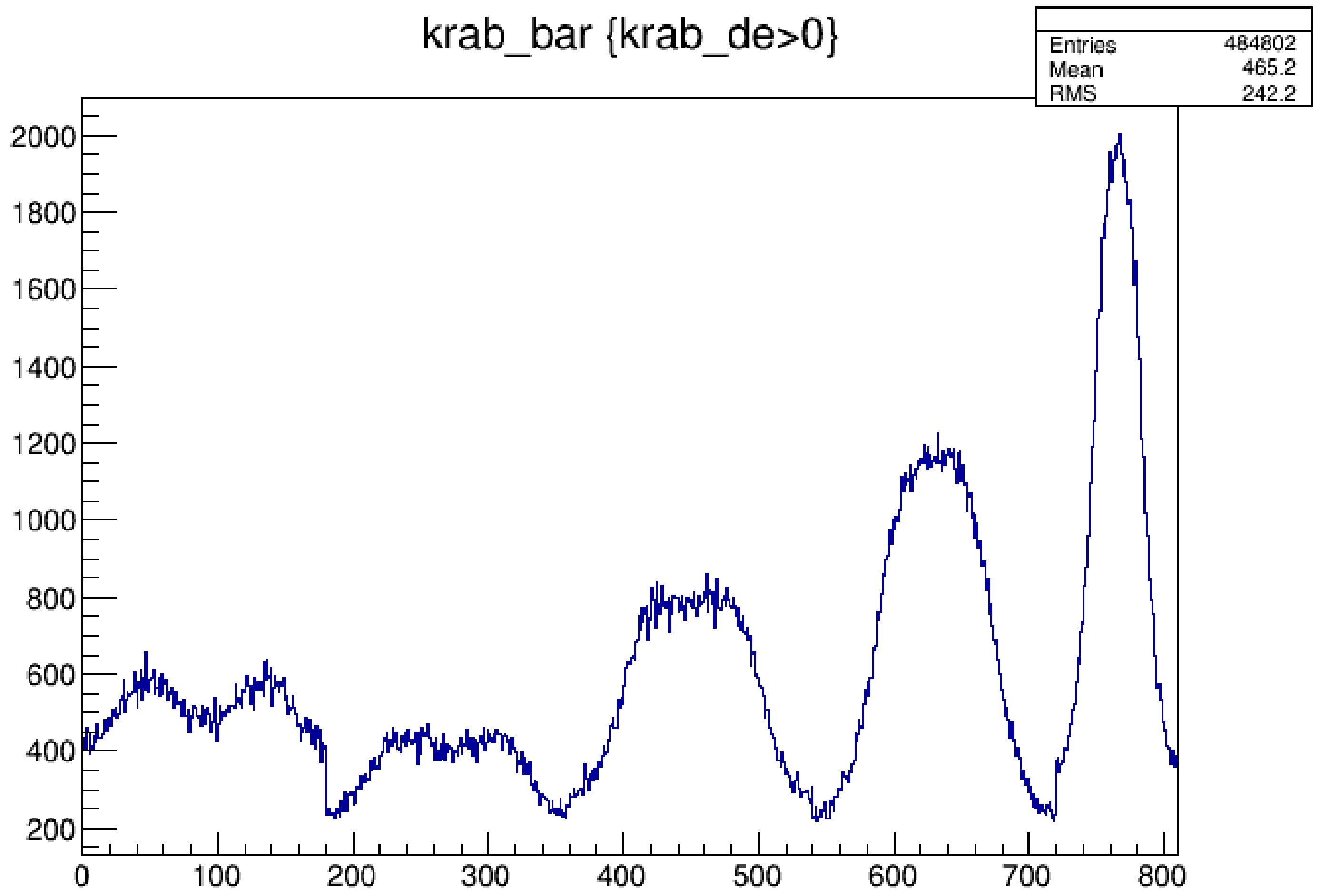

SciFi segment number

Summary & Conclusions

- **ASY-EOS measurements yield a moderately soft to linear density dependence of the symmetry energy:**
  $\gamma = 0.72 \pm 0.19$ (L= 72 ± 13 MeV).

- **First analyses using the LIGO and VIRGO constraints yield**
- **$\sim 10 < R_{NS}(1.4\ M_{\odot}) < \sim 13$ km → 26 < L < 84 MeV , which support the results of Lattimer and Steiner analysis of qLMXB**
  ($10.9 < R_{NS}(2.0\ M_{\odot}) < 12.7$ km) → 41 < L < 83 MeV, and
  is compatible with the ASY-EOS measurement.

- **The FOPI-LAND and ASY-EOS high energy results for L locate above the average for the low density measurements what seems to indicate a transition towards more stiff symmetry energy above the ρ_0.**

- **A precise measurement needed at ~1 AGeV to explore densities at 2-3 ρ_0.**

- **KRAB detector under construction.**

reviews:

Ph. Chomaz, F. Gulminelli, W. Trautmann, S.J. Yennello,
Eur. Phys. J. A 30 (2006).

M. B. Tsang et al.
Phys. Rev. Lett. 102, 122701 (2009)

M.B. Tsang et al.,
Phys. Rev. C 86, 015803 (2012).

W. Trautmann, H.H. Wolter,
Int. J. Mod. Phys. E21, 1230003 (2012).

B.-A. Li, À. Ramos, G. Verde, I. Vidaña,
Eur. Phys. J. A 50 (2014).

C J Horowitz et al.
J. Phys. G: Nucl. Part. Phys. 41 (2014) 093001

M. Baldo, G.F. Burgio, The nuclear symmetry energy,
Prog. Part. Nucl. Phys., 91 (2016) 203

Oertel, M., Hempel, M., Kl¨ahn, T., & Typel, S**.**
Rev. Mod. Phys., 89, 015007 (2017)

B.-A. Li, Nuclear Symmetry Energy Extracted from Laboratory Experiments,
Nucl. Phys. News, 27 (2017) 7

Nai-Bo Zhang, Bao-An Li, Jun Xu
Combined Constraints on the Equation of State of Dense Neutron-Rich Matter from Terrestrial Experiments and Observations of Neutron Stars,
arXiv:1801.06855v1

J. Piekarewicz Nuclear Astrophysics in the New Era of Multimessenger Astronomy
arXiv:1805.04780v1

Flows of light charged particles in Au (400 MeV/u) + Au reactions: KRATTA vs FOPI results

Fourier decomposition of the azimuthal distributions with respect to the reaction plane (ϕ_R) :

$$\frac{dN}{d(\phi - \phi_R)} = \frac{N_0}{2\pi}\left(1 + 2\sum_{n\geq 1} v_n \cos n(\phi - \phi_R)\right)$$

$v_1 \equiv \langle\cos(\phi - \phi_R)\rangle$ directed flow

$v_2 \equiv \langle\cos 2(\phi - \phi_R)\rangle$ elliptic flow

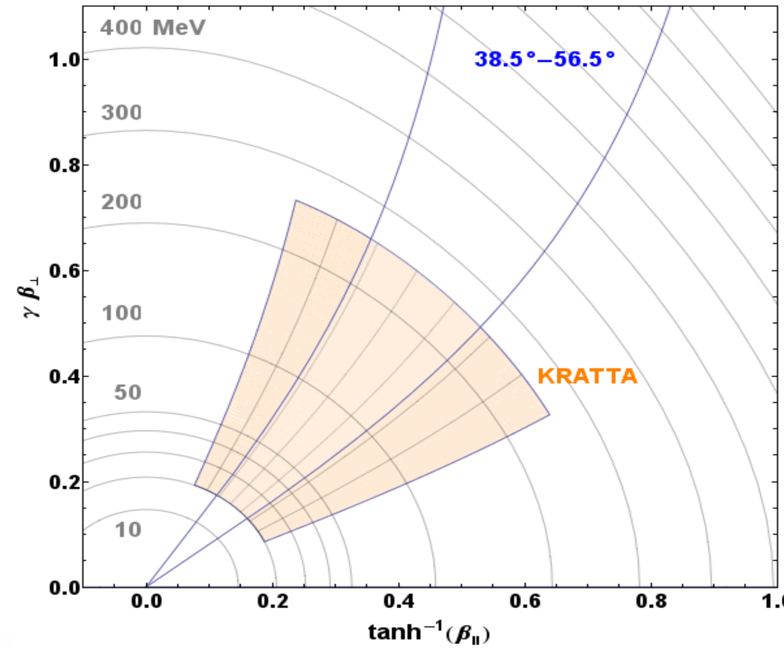

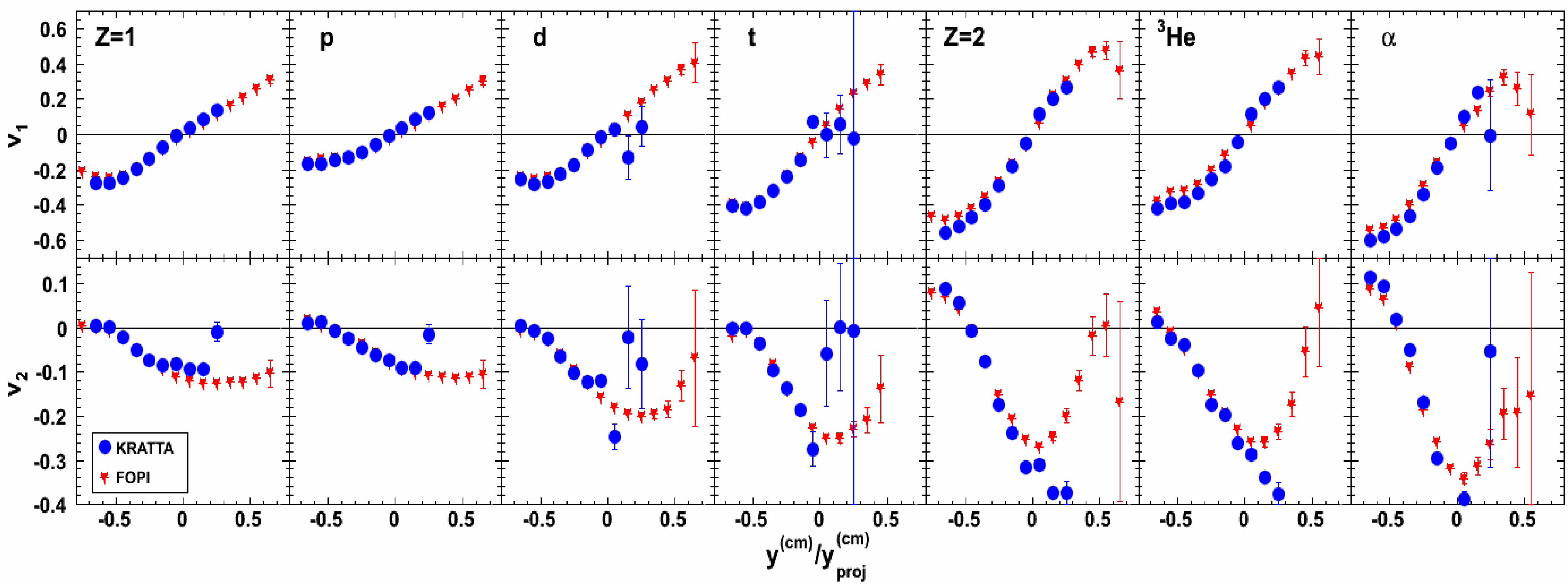

S. Kupny, PHD thesis, Jagiellonian University, Kraków (2016)

Model simulations

UrQMD Q. Li, J.Phys. G 31(2005)1359

„Fermi-gas" parametrization of the symmetry term:

$$E_{sym} = E_{sym}^{pot} + E_{sym}^{kin} = 22\ \text{MeV}\left(\frac{\rho}{\rho_o}\right)^{\gamma} + 12\ \text{MeV}\left(\frac{\rho}{\rho_o}\right)^{2/3}$$

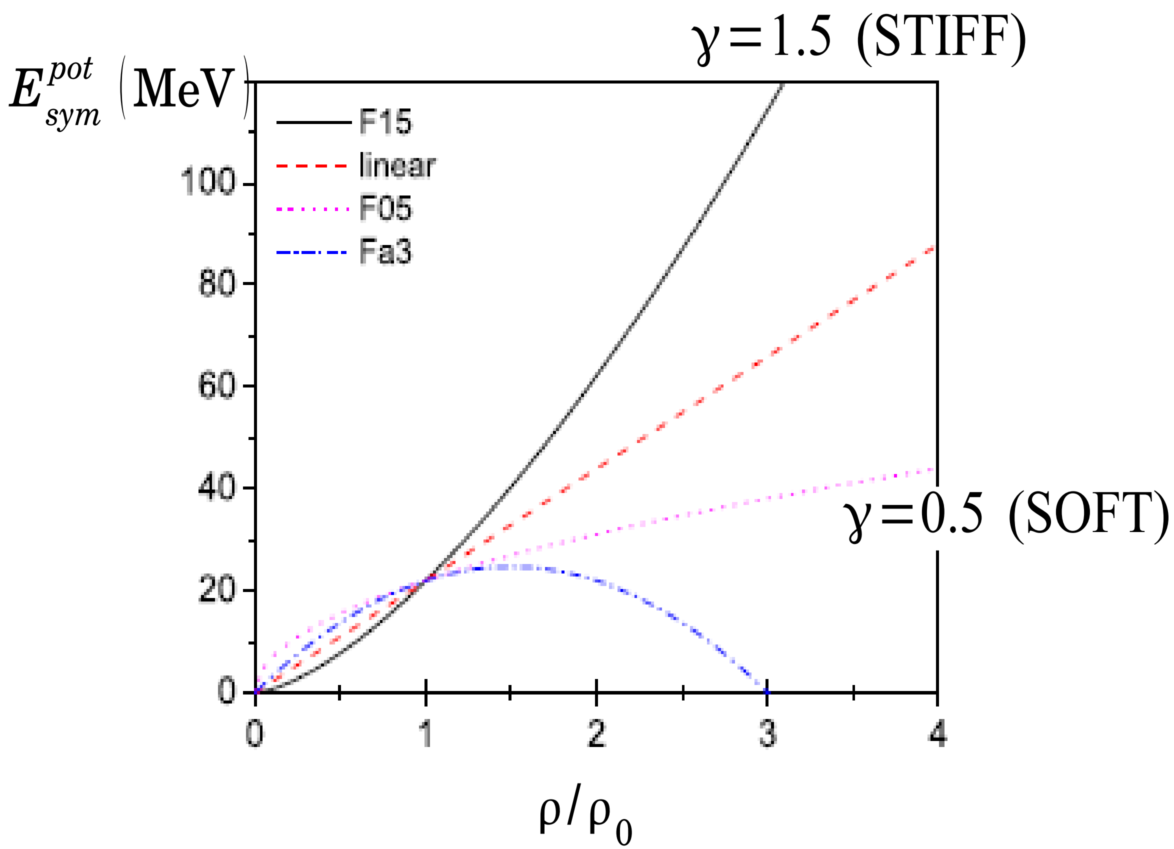

Stopping time = 150 fm/c

Nucleons → $\{\vec{r}_i, \vec{p}_i\}$

Clustering procedure

($\Delta r = 2.5$ fm, $\Delta p = 290$ MeV/c)

($\Delta r = 3$ fm, $\Delta p = 100$ MeV/c)

⋮

Charge distribution Au (400 MeV/u) + Au

KRATTA data ⟷ UrQMD predictions

●

ASY - SOFT

ASY - STIFF

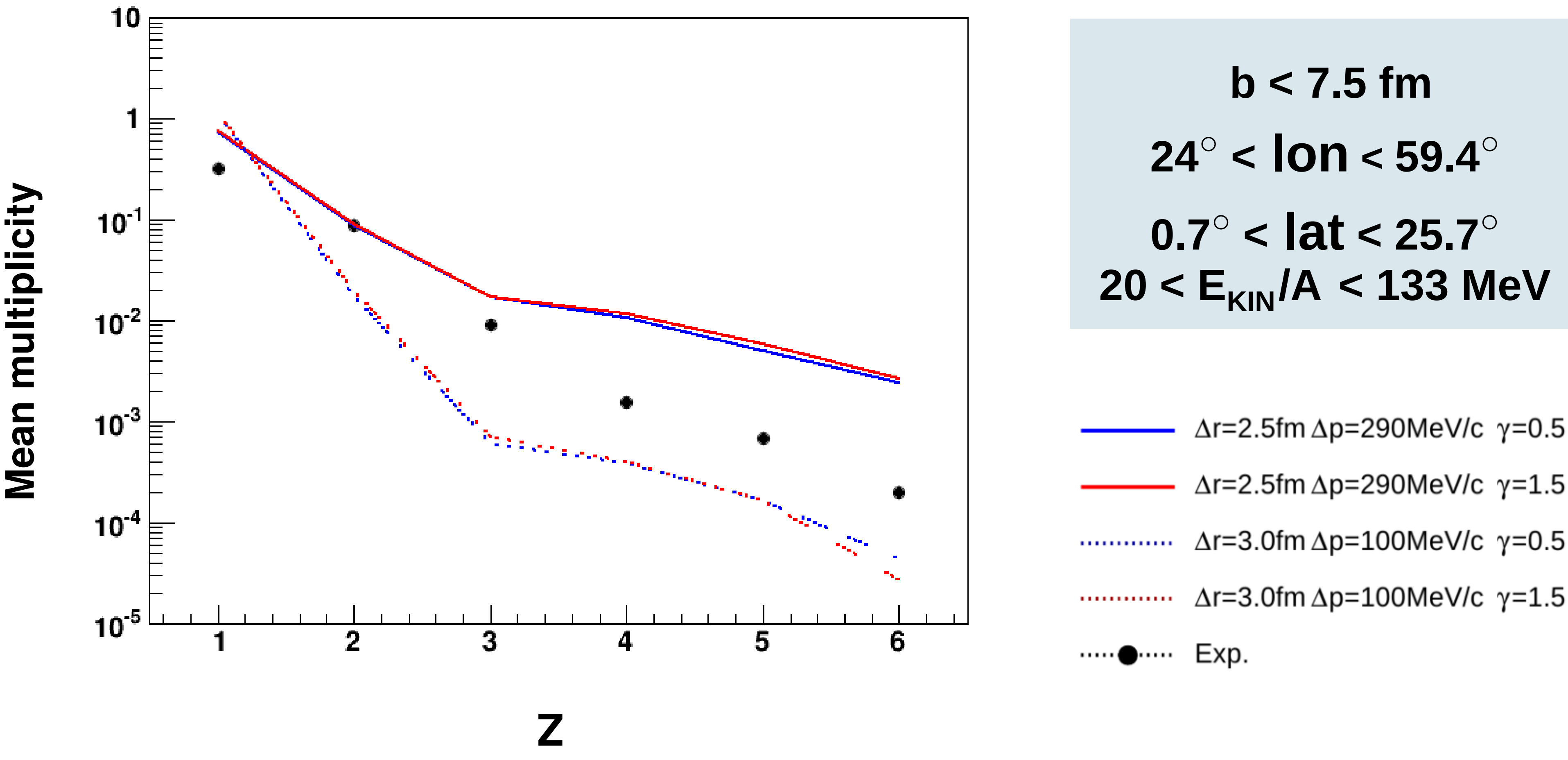

b < 7.5 fm

24° < lon < 59.4°

0.7° < lat < 25.7°

20 < E_{KIN}/A < 133 MeV

S. Kupny, PHD thesis, Jagiellonian University, Kraków (2016)

Energy/nucleon

Au (400 MeV/u) + Au

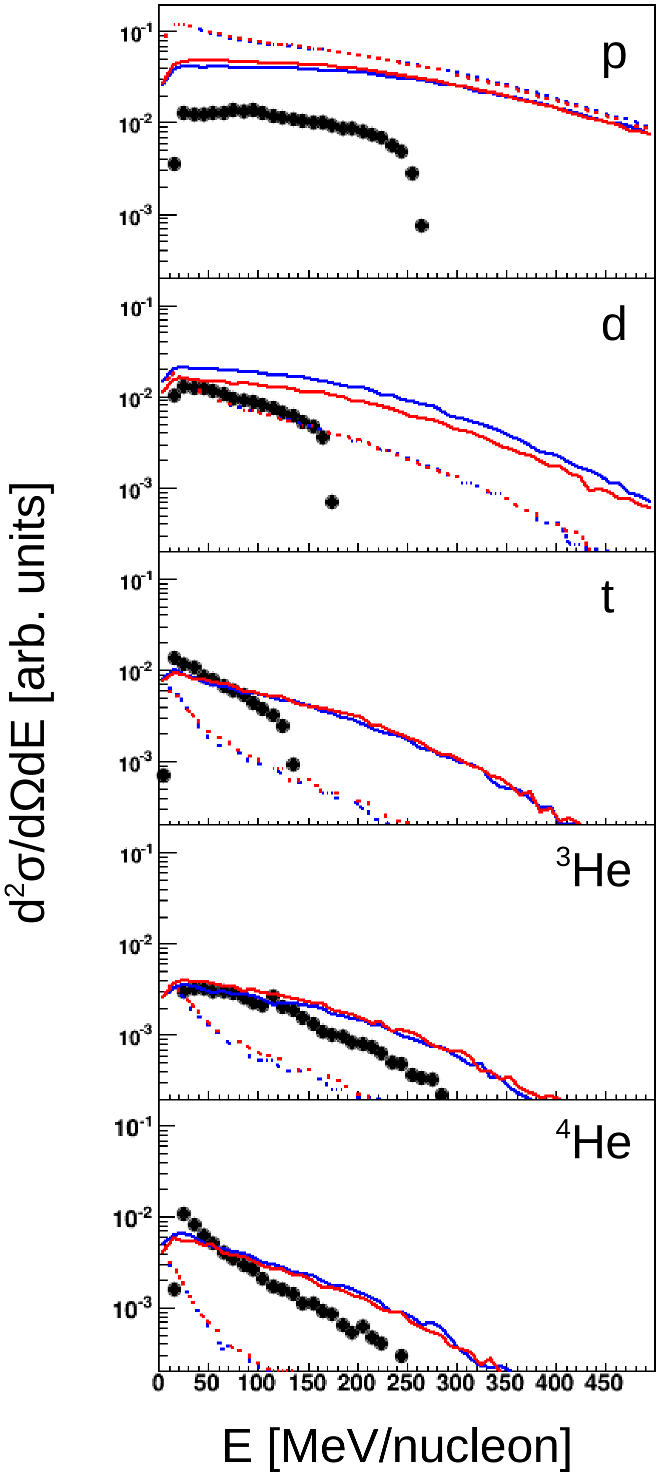

- Δr=2.5fm Δp=290MeV/c γ=0.5
- Δr=2.5fm Δp=290MeV/c γ=1.5
- Δr=3.0fm Δp=100MeV/c γ=0.5
- Δr=3.0fm Δp=100MeV/c γ=1.5
- Exp.

b < 7.5 fm

24° < lon < 59.4°

0.7° < lat < 25.7°

S. Kupny, PHD thesis, Jagiellonian University, Kraków (2016)

$t/^3He$ isotope ratios ($20 < E_{kin}/A < 133$ MeV)

Au (400 MeV/u) + Au
$5.5 < b < 7.5$ fm
$24^\circ < \Theta_{LAB} < 62^\circ$
$20 < E_{KIN}/A < 133$ MeV

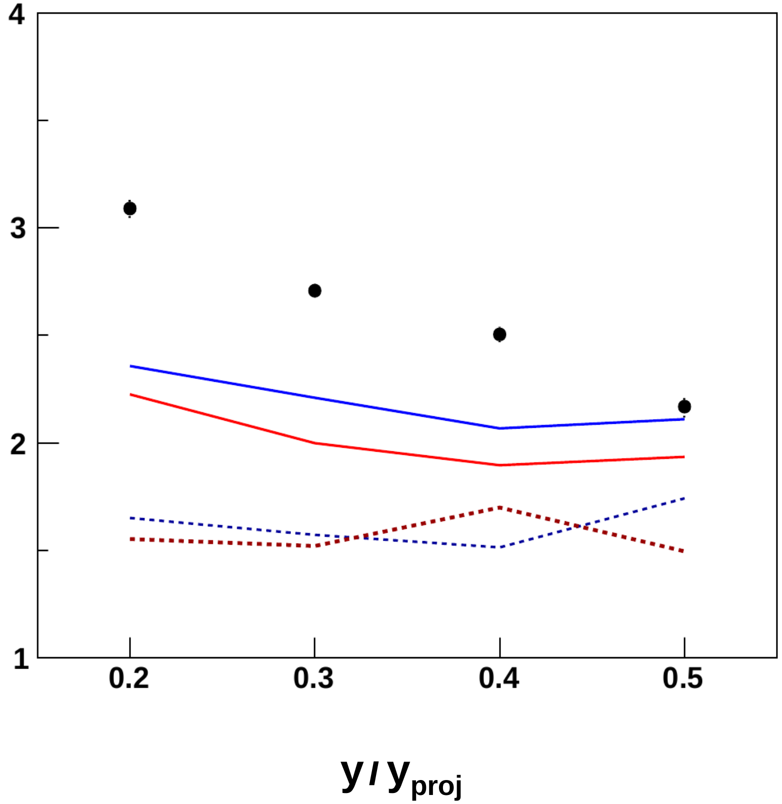

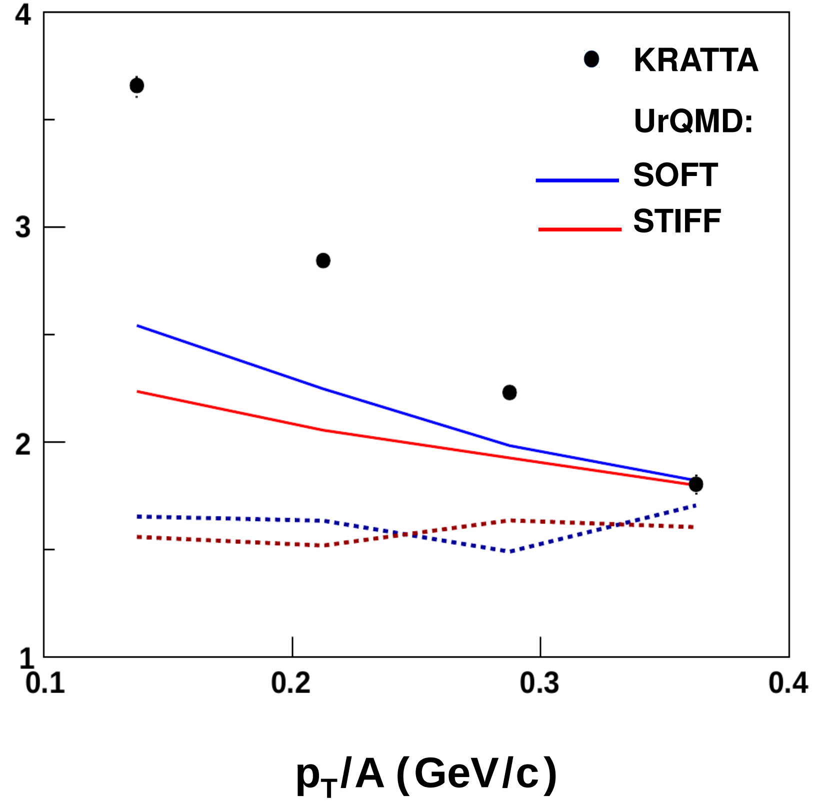

S. Kupny, PHD thesis, Jagiellonian University, Kraków (2016)

Proton flow (20 < E_{kin} < 250 MeV)

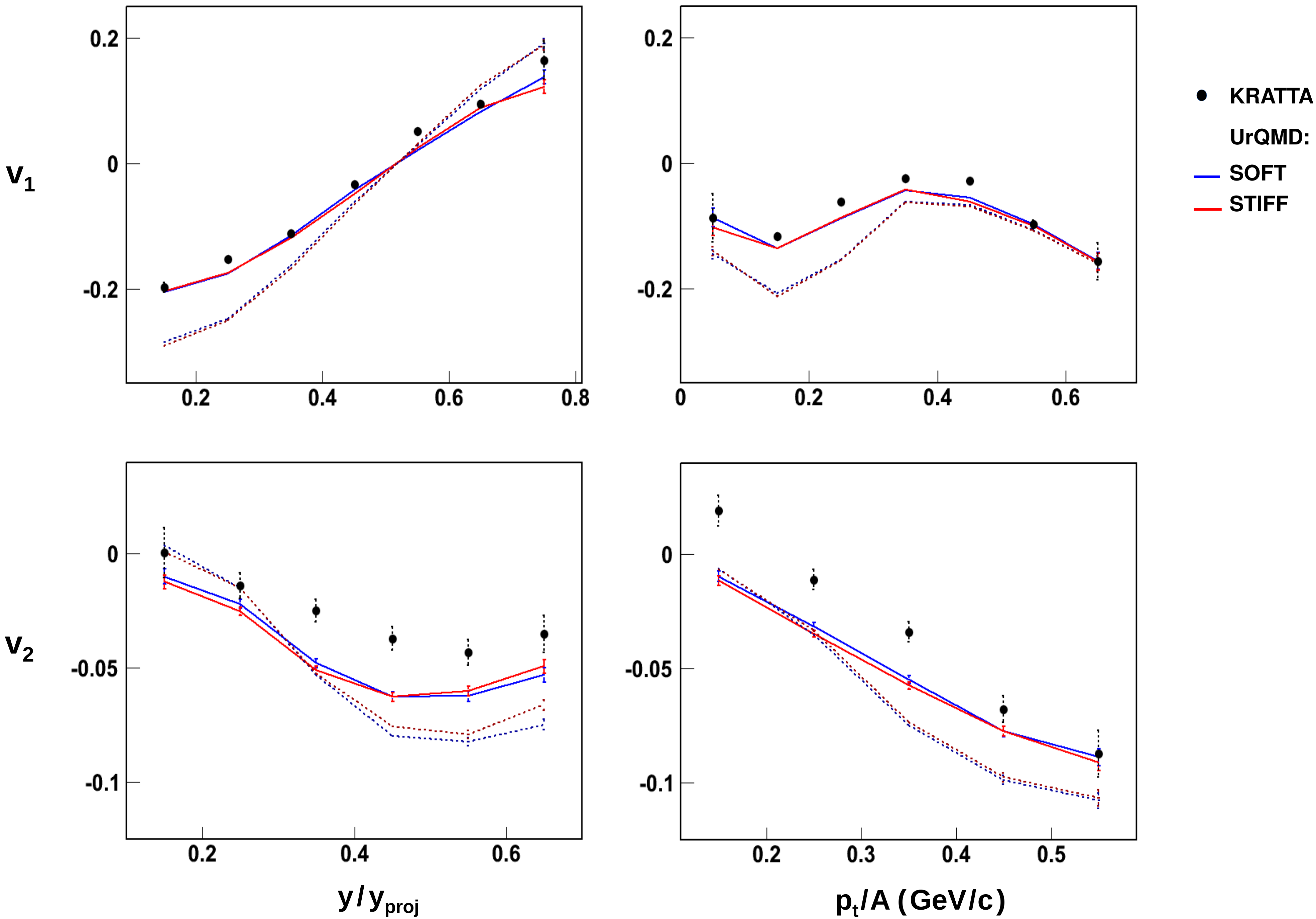

S. Kupny, PHD thesis, Jagiellonian University, Kraków (2016)

Deuteron flow $(20 < E_{kin}/A < 160\ \mathrm{MeV})$

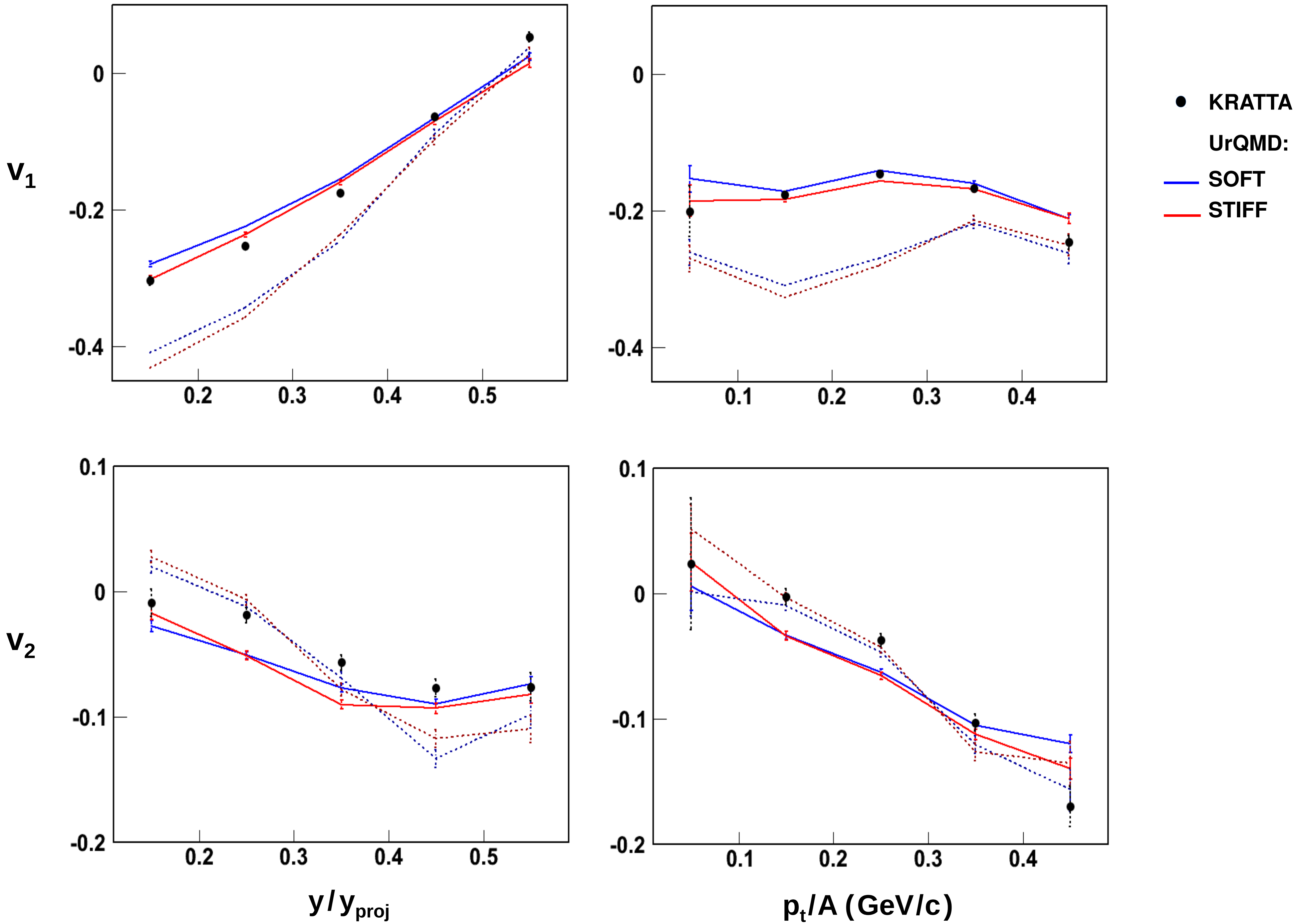

S. Kupny, PHD thesis, Jagiellonian University, Kraków (2016)

current status

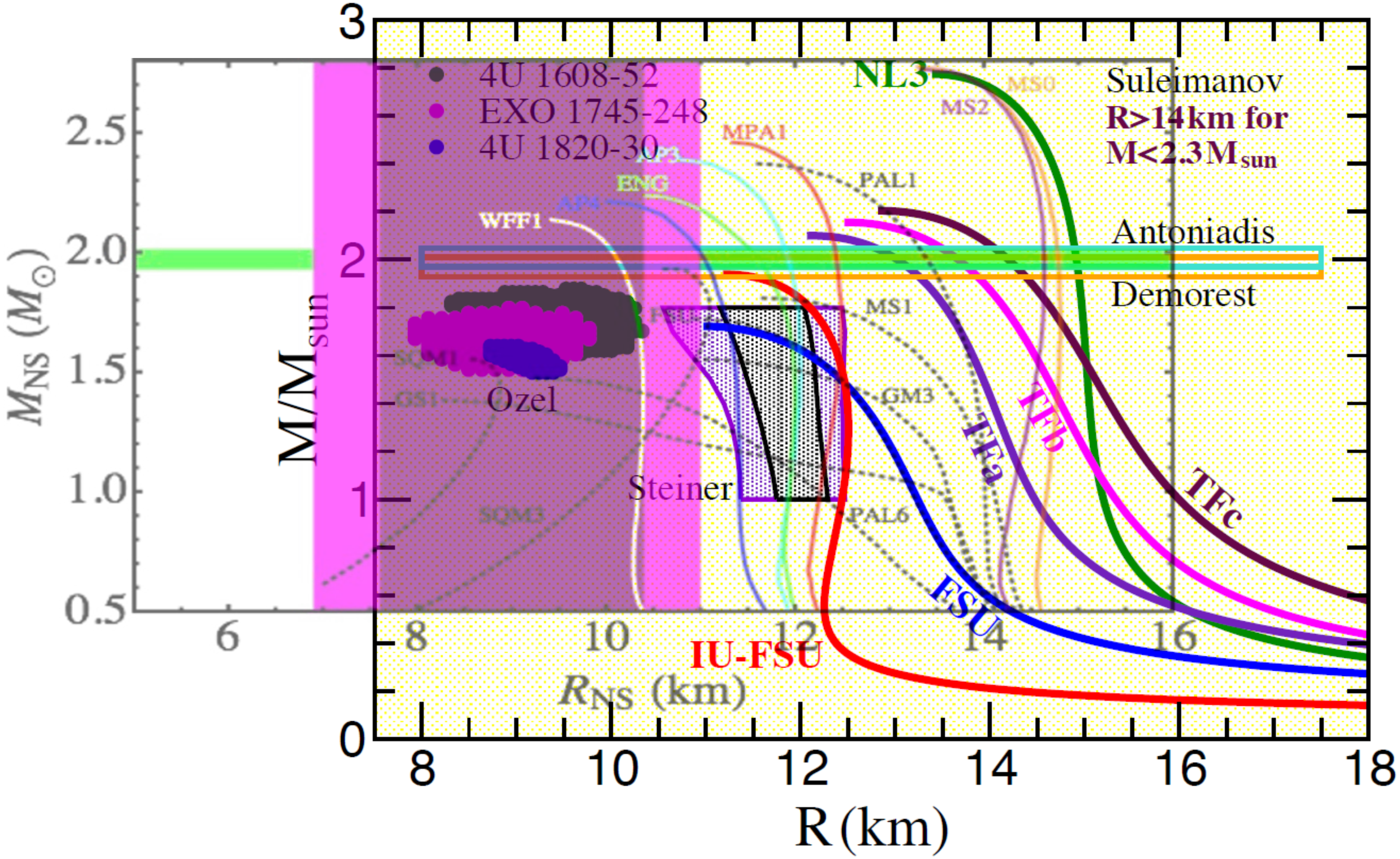

J. Piekarewicz, arXiv:1805.04780v1